

# 5 Chilean volcanoes

CHARLES R. STERN, HUGO MORENO, LEOPOLDO LÓPEZ-ESCOBAR (coordinators), JORGE E. CLAVERO, LUIS E. LARA, JOSE A. NARANJO, MIGUEL A. PARADA & M. ALEXANDRA SKEWES

There are over 200 Pleistocene and Holocene Andean arc volcanoes along western South America, occurring in four distinct segments (Fig. 5.1) called the Northern (NVZ; 2°N–5°S), Central (CVZ; 14°S–28°S), Southern (SVZ; 33°S–46°S) and Austral (AVZ; 49°S–55°S) volcanic zones. In the Andes of Chile alone there are more than 100 Pleistocene and Holocene stratovolcanoes, as well as a number of large volcanic fields and giant caldera complexes, of which 60 have documented Holocene eruptive activity (Simkin & Siebert 1994; González-Ferrán 1995). These are located in the CVZ of northern Chile, the SVZ of central-south Chile, and the AVZ of southernmost Chile. Pleistocene and Holocene backarc volcanic centres, the westernmost part of the Patagonian plateau basalts, also occur in southern Chile along the border with Argentina. In addition, intraplate oceanic volcanoes form Chilean islands in the Pacific Ocean, submarine volcanism takes place along the Chile Ridge, and slab-window volcanic activity occurs above the region where the Chile Ridge is currently being subducted, both along the west coast of Chile and in the submarine environment near the trench.

Pleistocene and Holocene volcanoes of the Chilean Andes provide a natural laboratory for the study of volcanism, magma genesis and volcanic hazards in the context of oceanic–continental plate collision. Andean volcanic activity results from subduction of the Nazca and Antarctic oceanic plates below the continental lithosphere of western South America (Fig. 5.1). Volcanoes in the CVZ of northern Chile and the SVZ of central-south Chile occur where the angle of subduction of the Nazca Plate is relatively steep ( $>25^\circ$ ) at depths  $>90$  km. These two active arc segments are separated by the Pampean flat-slab segment, below which subduction angle decreases and becomes relatively flat ( $<10^\circ$ ) at depths  $>90$  km. The northern boundary of the SVZ corresponds to the locus of subduction of the Juan Fernández Ridge of volcanic oceanic islands. At the southern end of the SVZ, the eastern extension of the Chile Ridge, which separates the Nazca from the Antarctic plate, is being subducted below South America, and the Patagonian gap in volcanism is observed between the SVZ and AVZ. These relations imply a clear genetic connection between plate subduction and volcanism that is confirmed by geochemical studies indicating that generation of Andean magmas is initiated by dehydration and/or melting of subducting oceanic lithosphere and interaction of these slab-derived fluids/melts with the overlying mantle wedge. Continental crust is incorporated into Andean magmas by a combination of subduction of crust into the subarc mantle and the assimilation of crust into mantle-derived magma.

Detailed studies of individual Andean volcanoes in Chile indicate that there is no unique ‘Andean-type’ volcanic arc (Stern 2004). The diversity of Pleistocene and Holocene Andean volcanoes and volcanic rocks in Chile, and the corresponding potential for different types of volcanic hazards, reflect a variety of magma genesis processes that need to be

evaluated in the context of both along-arc and across-arc variations in the geological and tectonic character of the continental South American Plate, the oceanic plates it is colliding with, and aspects of the collision process. Characteristics of the continental lithosphere, including pre-Andean basement ages, Andean structural evolution, crustal thickness and composition, and Neogene continental tectonic regimes vary significantly from north to south along the length of Chile, and these influence the genesis and fine structure of the Andean Pleistocene and Holocene volcanic arc in Chile. Both rates and directions of convergence differ north and south of the Chile Ridge triple-junction (Fig. 5.1). The age of the oceanic lithosphere being subducted also varies from north to south along-strike of the Chilean continental margin, as does depth of the trench. The amount and type of sediment in the trench changes as the result of north to south differences in climate, which have affected sediment supply to the trench since Miocene times (Alpers & Brimhall 1988). This, in turn, influences rates of sediment subduction and subduction erosion of the continental margin (Scholl *et al.* 1980), degree of hydration and consequently shear stress in the subduction zone (Ruff 1989), dynamics of mountain building (Giese *et al.* 1999; Lamb & Davis 2003), as well as Andean magma chemistry in different segments of the Chilean Andes (Stern 1991b, 2004).

This chapter describes Pleistocene and Holocene Andean volcanoes, volcanic hazards and magma genesis in Chile in the context of these tectonic and geologic variables, as well as other volcanic activity in Chile that occurs in a variety of tectonic settings.

## CVZ volcanoes of northern Chile (J.E.C., J.A.N. & C.R.S.)

Volcanoes of the Central Volcanic Zone (CVZ; Figs 5.1 & 5.2) are located in the Central Andes of southeastern Peru, western Bolivia, northern Chile and northwestern Argentina. In total, more than 1100 volcanic vents and/or edifices have been identified in the CVZ of the Andes (de Silva & Francis 1991). However, due to the hyperarid conditions that have prevailed in the region during the Pleistocene and Holocene, erosion has been minimal and some of these are most likely pre-Pleistocene in age. The hyperarid conditions result in excellent exposures of extremely well preserved volcanic features, and for these reasons studies of the evolution of CVZ centres in northern Chile have proved especially useful for understanding volcanic processes.

In northern Chile, Pleistocene and Holocene CVZ volcanoes form an essentially continuous chain between Tacora volcano, located near the Peru–Chile border at 17.5°S, to the Nevado Ojos del Salado volcanic complex at 27°S, the world’s highest active volcano summit (6886 m; Simkin & Siebert 1994).

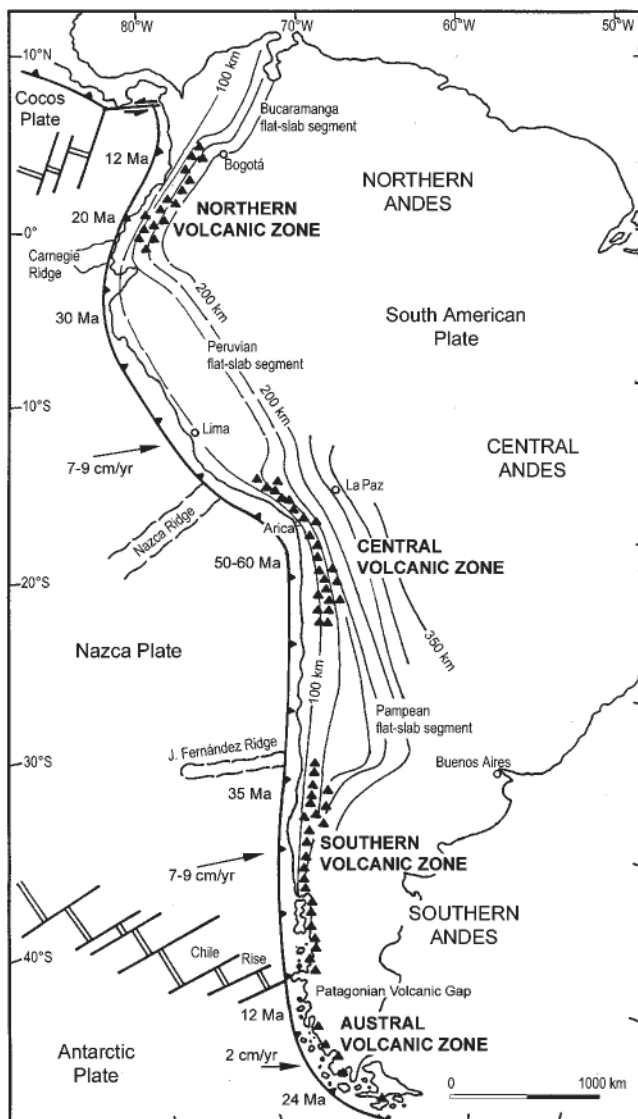


**Fig. 5.1.** Schematic map, modified from Stern (2004), of the four volcanically active zones in the Andes, subduction geometry as indicated by depth (in km) to the Benioff zone, oceanic ridges, ages of oceanic plates close to the trench, and convergence rates and directions along the length of the Andes. Andean volcanoes in Chile occur in the Central, Southern and Austral volcanic zones.

Most of the >30 large stratovolcano complexes that form the Chilean part of the CVZ occur along the border between Chile and Bolivia or Argentina, but a few centres along the volcanic front, such as Taapaca, San Pedro and Láscar (Fig. 5.2) are located completely in Chile. The Chilean part of the CVZ includes the giant La Pacana caldera (Gardeweg & Ramírez 1987; Lindsay *et al.* 2001a, b; Schmitt *et al.* 2001, 2002), and many of the Chilean CVZ stratovolcanoes and smaller caldera complexes occur within the area covered by the ignimbrites of the Altiplano–Puna Volcanic Complex (Fig. 5.2; de Silva 1989a, b). A number of small pyroclastic cones, lava flows, isolated domes and maars also form minor eruptive centres in the Chilean part of the CVZ. Although many of the volcanoes of the Chilean CVZ are remote from large population centres and present no significant direct volcanic hazard, explosive eruptions can be very hazardous for air safety and threaten populated areas in northwestern Argentina and/or western Bolivia.

### Geological and tectonic setting

Volcanoes of the CVZ result from subduction of the Nazca Plate below the Central Andes (Figs 5.1 & 5.2). The northern end of the CVZ is located in Peru at 14°S, where subduction of the Nazca Ridge results in a dramatic decrease in subduction angle below the Peruvian flat-slab segment to the north. The southern margin of the CVZ, where the Tres Cruces–Nevado Ojos del Salado volcanic chain is located, coincides with a seismic discontinuity at 27°S (González-Ferrán *et al.* 1985), superimposed on a gradual decrease in subduction angle associated with the Pampean flat-slab segment to the south, where Pleistocene and Holocene magmatism is absent (Kay & Mpodozis 2002). Convergence velocity between the Nazca and South American plates in northern Chile is 7.8–8.4 cm/year (DeMets *et al.* 1990). Obliquity of the convergence angle varies between 0° at the latitude of Arica (18°S; Fig. 5.2) to c. 24° west of the southern margin of the CVZ. The age of the oceanic Nazca Plate being subducted below northern Chile is <60 million years (Fig. 5.1). Subduction angle as defined by the Wadati–Benioff zone is c. 25° (Cahill & Isacks 1992), and below northern Chile the subducted plate descends to a depth of >400 km (Dorbath *et al.* 1996). The volcanic front of the CVZ is located approximately 120–150 km above the subducted slab and 260–340 km east of the Peru–Chile Trench, which is >7000 m deep everywhere west of the CVZ and reaches a maximum depth of 8055 m below sea level at 23°S. The trench is devoid of sediment (Thornburg & Kulm 1987a) because of the hyperarid conditions in northern Chile (Hartley *et al.* 2000; Hartley 2003).

Most of the Pleistocene and Holocene volcanic centres in the CVZ of northern Chile occur along the western boundary of two morphotectonic regions of the Central Andes referred to as the Altiplano (15–23°S) and Puna (23–28°S). Both these regions include a high central plateau, at an elevation of 3700 to 4200 m above sea level, bounded by Eastern and Western Cordilleras, with numerous peaks reaching >6000 m elevation. They occur above the thickest crust on Earth: 60–65 km thick below the Altiplano and Puna plateaux and >70 km thick below the bounding mountain belts (James 1971; Beck *et al.* 1996). The present-day topography of the Altiplano and Puna is essentially the result of the last Andean orogenic or deformation episode, known in the literature as the ‘Quechua Phase’ (Noble *et al.* 1997). This widely recognized episode has been dated as beginning at c. 27 Ma in the Eastern Cordillera (Semperé *et al.* 1990; Hérail *et al.* 1996) and more recently in the Western Cordillera (Muñoz & Charrier 1996; García *et al.* 1999a; Wörner *et al.* 2000c). This deformation resulted from an increase in the rate of subduction below the Central Andes at c. 27 Ma, which also produced the generation of large volumes of magmas of different compositions (Sébrier & Soler 1991), although the onset of volcanism from this event was not simultaneous along the whole Central Andes. Very thick crust below the Central Andes may be due to either crustal shortening (Isacks 1988; Beck *et al.* 1996; Allmendinger *et al.* 1997; Kley *et al.* 1999), magmatic underplating (Tosdal *et al.* 1984; Schmitz *et al.* 1997, 1999), or a combination of the two, with more crustal shortening in the Eastern Cordillera (Cordillera Oriental) and more magmatic underplating and lithospheric hydration below the Western Cordillera (Cordillera Occidental; James 1971; James & Sacks 1999; Giese *et al.* 1999; Victor *et al.* 2004).

The CVZ also occurs above some of the oldest crust along the west coast of South America, exposed as the Palaeoproterozoic (2.0–1.8 Ga) metamorphic and igneous rocks of the Arequipa terrane of southern Peru. Metamorphic rocks with similar protolith ages have also been reported in the Antofalla basement exposed at Belén, Chile, implying that such rocks may underlie a large part of the CVZ of northern Chile (Wörner *et al.* 2000c). Protoliths in these terranes may be either parautochthonous (Perigondwanan) and related to the Brazilian craton (Tosdal 1996), or allochthonous and part of the Grenvillian province of Laurentia (Dalziel 1994, 1997; Wasteneys *et al.*

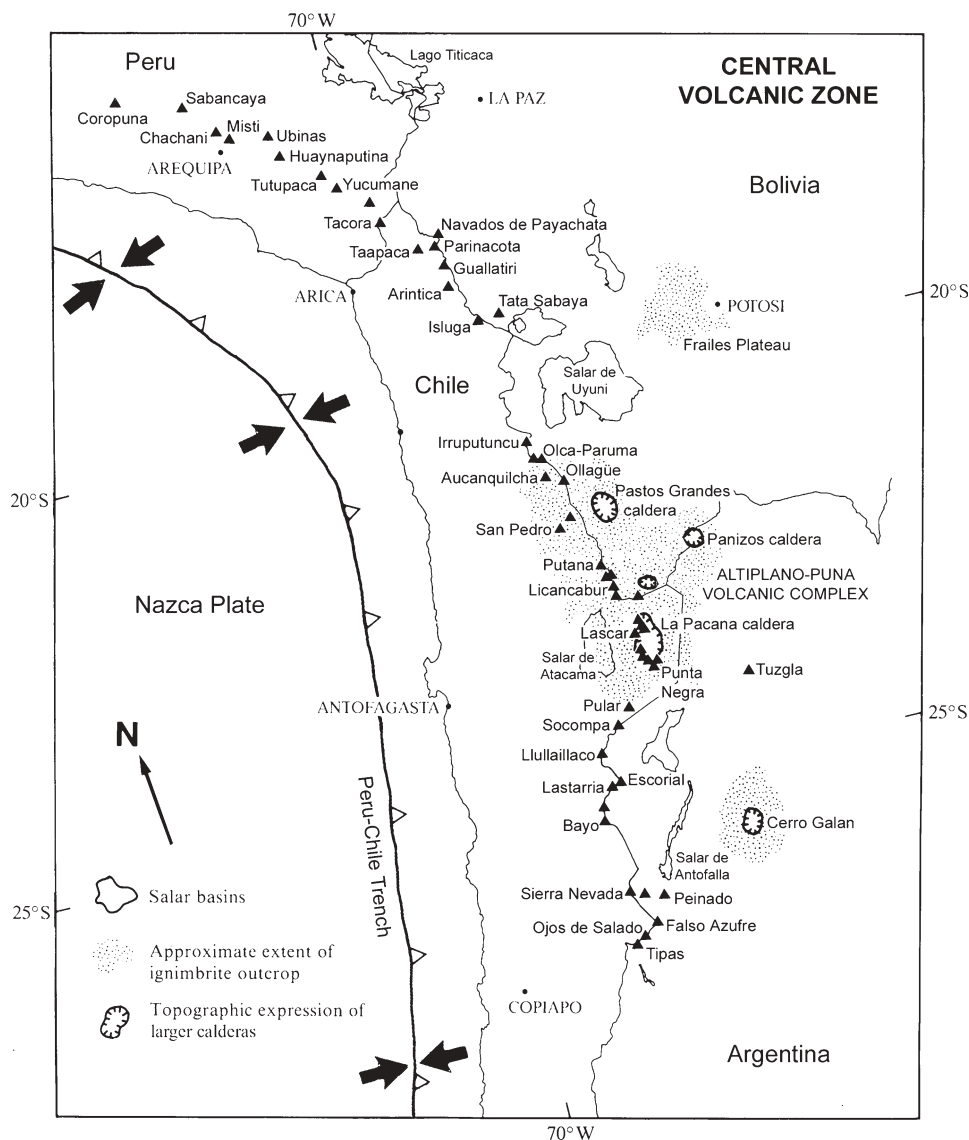


Fig. 5.2. Schematic map of the location of some of the larger volcanoes and caldera systems in the CVZ.

1995; Loewy *et al.* 2004). Rocks with 'Grenvillian' (1.3–1.0 Ga) protolith ages also occur at Choja in northern Chile (Loewy *et al.* 2004). These Proterozoic rocks were subsequently affected by the Neoproterozoic to Early Palaeozoic (680–510 Ma) Pampean igneous and metamorphic event, first identified in the basement further south in the Sierras Pampeanas ranges in Argentina (Rapela *et al.* 1998a, b), as well as younger Palaeozoic (470–340 Ma) events (Wörner *et al.* 2000c; Jaillard *et al.* 2000; Ramos & Alemán, 2000; Lucassen *et al.* 2001a). South of the Antofalla basement, below the southern part of the CVZ, accretion and amalgamation of the Oaxaquia, Famatina, Cuyania and Chilenia allochthonous terranes took place during the Palaeozoic (Ramos *et al.* 1986; Pankhurst & Rapela 1998; Ramos & Alemán 2000; Astini & Dávila 2002, 2004; Loewy *et al.* 2004).

A notable and significant aspect of the western margin of northern Chile is the total lack of Mesozoic and Cenozoic arc–trench gap accretionary complexes, and the occurrence of pre-Andean Proterozoic to Early Mesozoic exotic and parautochthonous terranes along the coast (Rutland 1971; Kulm *et al.* 1977; Schweller & Kulm 1978). This is interpreted to result from subduction erosion, or rasping off of the continental

margin by a combination of both continental slope retreat and erosion of the underside of the upper plate (Rutland 1971; Scholl *et al.* 1980; Ziegler *et al.* 1981; von Huene & Lallemand 1990; Stern 1991b; von Huene & Scholl 1991, 1993; Lallemand *et al.* 1992a, b; Lallemand 1995; von Huene *et al.* 1999, 2004; von Huene & Ranero 2003; Sallarés & Ranero 2005). Other geological evidence for subduction erosion along the west coast of northern Chile includes the *c.* 250 km eastward migration of the Andean Jurassic to Cenozoic magmatic belts (Ziegler *et al.* 1981; Peterson 1999; Giese *et al.* 1999), the NW strike and almost complete disappearance north of 27°S of the Late Palaeozoic Gondwanan subduction accretionary complexes that form the Coastal Cordillera in central Chile (Stern 1991b; Stern & Mpodozis 1991), and shortages in the amount of crustal shortening that can be accounted for by crustal area balance calculations (Schmitz 1994).

The suggested mechanism for slope retreat is continental margin collapse towards the trench caused by extensional faults, generating debris that are pushed into the horst and graben structures on the subducting oceanic plate, which resemble the teeth of a chain saw (Hilde 1983; von Huene *et al.* 2004). Such structures and processes have been well



documented along the continental margin of southern Peru (Lallemant *et al.* 1992a, b; Hampel *et al.* 2004a, b) and northern Chile (Delouis *et al.* 1996, 1998; von Huene *et al.* 1999; Hartley *et al.* 2000; von Huene & Ranero 2003; González *et al.* 2003; Lovelace *et al.* 2005; Sallarés & Ranero 2005). Rates of subduction erosion depend on factors such as subduction angle, sediment supply to the trench, and subduction of buoyant features such as ridges (Scholl *et al.* 1980; Shreve & Cloos 1986; Ruff 1989; Bangs & Cande 1997; Lamb & Davis 2003). Both low angle subduction and low sediment supply to the trench, features of the plate boundary west of northern Chile, are factors that enhance the potential for increased rates of subduction erosion. Here the Peru–Chile trench receives almost no sediment from the few mountain glacier-fed drainage systems that cross the Atacama Desert (Thornberg & Kulm 1987a; Hartley 2003).

Long-term average rates of subduction erosion west of the Central Andes may be as high as 40 km<sup>3</sup> of crust per million years per kilometre of trench in order to have removed an estimated 250 km of 40-km-thick crust in the last 25 million years of near-orthogonal convergence (Ziegler *et al.* 1981; Lallemant 1995). This is equivalent to 4% of the volume of subducted oceanic crust in the same time period, which is well within the carrying capacity of the underthrusting grabens entering the subduction zone below northern Chile (von Huene & Ranero 2003). This subducted crust may have an important influence on the extent to which the subducted slab is hydrated (Giese *et al.* 1999; Ranero & Sallarés 2004), the dynamics of the interaction between the subducting oceanic and overlying continental plate (Ruff 1989; Lamb & Davis 2003), and on the chemistry of CVZ magmas in northern Chile (Stern 1991b, 2004; Kay *et al.* 1999; Macfarlane 1999).

Subduction erosion and decreasing subduction angle have caused the Andean magmatic arc to migrate into its current position in the Altiplano–Puna region. Large volumes of rhyolitic magmas started to erupt here at *c.* 27 Ma, most of them probably associated with large calderas, forming extensive ignimbritic plateaux to the west of the Altiplano. During the Miocene epoch a series of medium to large andesitic to dacitic stratovolcanoes was formed. Magmatic activity increased dramatically approximately 10 million years ago (Allmendinger *et al.* 1997). In the late Miocene and Pliocene, new stratovolcanoes of the same compositions were formed, as well as large-volume rhyodacite ignimbrites, such as the Lauca, Purico, Atana and Toconce ignimbrites (Gardeweg & Ramírez 1987; Kött *et al.* 1995; Wörner *et al.* 2000b; Lindsay *et al.* 2001a, b; Schmitt *et al.* 2001; García *et al.* 2004). Due to the hyperarid conditions in northern Chile, many of these volcanic centres and ignimbrites are extremely well preserved. The recent CVZ volcanic chain was formed during Late Pleistocene to Holocene times, with magmas mainly of the same compositions as in the Miocene and Pliocene.

### CVZ volcanoes and hazards

Late Pleistocene to Holocene volcanism in northern Chile has been characterized by the formation of both andesitic stratovolcanoes and dacitic dome complexes, with associated pyroclastic flow, tephra fallout, debris avalanche and block-and-ash flow deposits. Less common are small monogenetic andesitic to basaltic andesite eruptive centres, such as the Ajata flank centres of Parinacota volcano, La Poruña pyroclastic cone on the lower western flank of Ollagüe volcano and La Poruña pyroclastic cone and associated lava on the western flank of San Pedro volcano. A small number of isolated high-silica dacitic to rhyolitic flows, some forming ‘torta’-type domes, have been recognized locally, such as the Chao (de Silva *et al.* 1994) and Tocorpuri (de Silva & Francis 1991) domes in Chile, and others in Bolivia (Watts *et al.* 1999). Large caldera complexes, including the giant La Pacana system in Chile and

others in southwestern Bolivia and northwestern Argentina, have produced the Pliocene and Pleistocene ignimbrites of the Altiplano–Puna Volcanic Complex that crop out in northern Chile.

Although most of the active volcanoes of northern Chile are located in remote areas, with few people living nearby, future eruptions of some of them could affect inhabited areas located in southwestern Bolivia and/or northwestern Argentina, as was the case during the 1993 eruption of Lascar volcano (Gardeweg & Medina 1994). Also, although low-altitude prevailing winds in the area blow generally from west to east, high-altitude winds may blow from east to west in some seasons. Therefore, tephra falls from large eruptions could disperse to the west into Chile and affect both the local population and wetlands (bofedales), which are the main feeding area of altiplanic camelids (llamas and alpacas), and therefore damage the local economy (Castellaro *et al.* 2004).

Some of the largest, most active and better studied of the many Late Pleistocene to Holocene CVZ volcanic centres in northern Chile (Fig. 5.2) include Tacora (Clavero *et al.* 2006); Parinacota (Wörner *et al.* 1988, 1992a; Clavero *et al.* 2002, 2004a), Taapaca (5850 m; Clavero *et al.* 2004b), Guallatiri (García *et al.* 2004), Arintica (5597 m), Isluga (5501 m), Irruputuncu (Clavero *et al.* 2005), Olca-Paruma (5450 m), Aucanquilcha (6176 m; Grunder *et al.* 2004), Ollagüe (Feeley *et al.* 1993; Feeley & Davidson 1994; Clavero *et al.* 2004c), Azufre (5846 m), San Pedro (Francis *et al.* 1974; O’Callaghan & Francis 1986), Putana (5890 m), Escalante (5971 m), Licancabur (5916 m; Figueroa 2001), Guayaques (5584 m), Colachi (5631 m), Acamarachi (6046 m), Aguas Calientes (5924 m), Lascar (Matthews *et al.* 1994, 1997, 1999; Gardeweg *et al.* 1998b), Chiliques (5778 m), Punta Negra (5852 m), Pular (6233 m), Socompa (Francis *et al.* 1985; van Wyk de Vries *et al.* 2001), Llullaillaco (Gardeweg *et al.* 1984; Richards & Villeneuve 2001), Escorial (5447 m), Lastarria (Naranjo, 1988, 1992; Naranjo & Francis 1987), Bayo (5401 m; Naranjo 1988), Sierra Nevada (6127 m; Clavero *et al.* 1997), Nevado Ojos del Salado (González-Ferrán *et al.* 1985; Baker *et al.* 1987b; Gardeweg *et al.* 1998a) and Nevado Tres Cruces (Gardeweg *et al.* 2000).

We briefly describe below a selection of the most important CVZ volcanoes, chosen according to criteria including their historic activity and/or prominent features such as the occurrence of debris avalanches or notable pyroclastic fans.

#### *Tacora volcano (17.7°S, 69.8°W, 5980 m)*

Located close to the Peru–Chile border, this is the northernmost active volcano in Chile. It has permanent fumarolic activity on its western flank. Although there are no reliable records of historic eruptive activity, unconfirmed reports suggest two eruptive events in 1930 and 1937 (Simkin & Siebert 1994). The volcanic edifice is formed by a series of lavas and domes, mainly of dacitic composition, although many andesite flows also occur, associated with block-and-ash flow deposits, located mainly on its southwestern flank. It has been active at least since the Middle Pleistocene (*c.* 720 ka; Clavero *et al.* 2006), with its more recent eruptive activity located on its upper western flank (*c.* 50 ka). It exhibits a permanent degassing activity, which mainly consists of CO<sub>2</sub> and SO<sub>2</sub>, also accompanied by seismic activity (Clavero *et al.* 2005). The edifice has suffered strong glacial erosion and is partially covered with moraines on its lower flanks. It also suffered a partial sector collapse of its southern flank, directed towards the south. This generated a debris avalanche deposit that partially inundated the Caracarani basin (Clavero *et al.* 2006).

#### *Parinacota volcano (18.2°S, 69.1°W, 6348 m)*

Located on the Chile–Bolivia border, this is a prominent young stratovolcano (Fig. 5.3) that has evolved in three main stages beginning in the late Pleistocene (Wörner *et al.* 1988, 2000b; Davidson *et al.* 1990; Clavero *et al.* 2002; 2004a; Hora *et al.*



**Fig. 5.3.** Nevados de Payachata volcanoes, with Parinacota volcano in front and Pomerape volcano behind, viewed from the south across Lake Chungará. Photo by J. Clavero.

2004). Although there are no records of historical eruptive activity, the whole of the new, almost perfect, volcanic cone has been built in the last 8000 years, and Aymara legends talk about hot clouds coming down from the volcano shortly before the Spanish arrived in the area. During its earlier stage (Parinacota 1, late Pleistocene, 300–40 ka) rhyolitic to andesitic magmas were erupted, forming a voluminous lava-dome complex with associated pyroclastic fans (mainly block-and-ash flow deposits), deposited in the Upper Lauca basin. It later evolved to a steep-sided composite stratocone (Parinacota 2, late Pleistocene–Holocene, 40–8 ka), mainly formed by andesitic and dacitic lava flows and scoria tephra fallout deposits. Around 8000 years ago this ancestral Parinacota volcano partially collapsed towards the west, inundating the upper Lauca basin in a single and catastrophic event that produced the Parinacota Debris Avalanche deposit (140 km<sup>2</sup> and 6 km<sup>3</sup>; Clavero *et al.* 2002, 2004a). Soon after the collapse a new stratocone started to build, with the emission of andesitic lava flows and pyroclastic flows and their associated fallout deposits (Holocene, <8 ka). Some lahars, mainly shed towards the south, west and east, were generated in Holocene times. Contemporaneously with the formation of the central cone, a series of flank cones and their associated basaltic andesite to andesitic lava flows were formed (Ajata centres, 6–1.4 ka; Entenmann 1994; Wörner *et al.* 2000b; Clavero *et al.* 2004a). The new cone (Parinacota 3 unit) has an estimated minimum volume of 18 km<sup>3</sup>, which gives a minimum eruption rate of 2.25 km<sup>3</sup>/ka for the last 8000 years, making Parinacota volcano one of the most active volcanoes in northern Chile during the Holocene.

#### *Taapaca Volcanic Complex (18.1°S, 69.5°W, 5850 m)*

Located on the western margin of the western Cordillera, this is a dacitic volcano (35 km<sup>3</sup>; Fig. 5.4) which has been active since at least the lower Pleistocene (Wörner *et al.* 2000b; Clavero *et al.* 2004b). Although it has no record of historical eruptions, it has had persistent effusive and explosive eruptive activities during both the late Pleistocene and Holocene (Clavero *et al.* 2004b). Volcanism has built a substantial volcanic complex, including a large partially eroded stratocone and a large dome complex. Four stages of evolution are recognized, with volcanism occurring in short bursts between much longer periods of dormancy. Apart from early poorly preserved silicic andesites in its first stage, Taapaca has generated remarkably similar porphyritic hornblende–biotite dacites with distinctive sanidine megacrysts for at least 1.5 Ma. The main products of the volcano are dacite lavas and domes with associated pyroclastic deposits, of which the most common ones are block-and-ash flow deposits. There have also been several sector collapses that have generated



**Fig. 5.4.** Taapaca volcano viewed from the SW. In the foreground is the town of Putre, which is built on top of Late Pleistocene and Holocene pyroclastic deposits derived from this volcano. Photo by J. Clavero.

debris avalanches. These were closely associated with volcanic blasts and episodes of dome growth. The main focus of volcanic activity has migrated 4–5 km towards the SW with time. Late Pleistocene to Holocene activity has involved at least three sector collapses of hydrothermally altered domes along the flanks of the stratocone. Volcanic blasts, block-and-ash flows, debris avalanches and lahars have been distributed down the southwestern flanks of the complex. These areas correspond to the main populated part of the Chilean Altiplano, including Putre, the largest town of the Chilean Precordillera (Fig. 5.4), and also the location of the main road between Bolivia and the Pacific coast. For this reason Taapaca is the most hazardous volcano in northern Chile, since a future eruption would certainly produce several of the recurrent volcanic hazards mentioned above and therefore threaten these areas.

#### *Guallatiri volcano (18.4°S, 69.2°W, 6071 m)*

Together with the Acotango, Humarata and Capurata centres, this forms a southward-younging north–south volcanic chain (García *et al.* 2004). Guallatiri is the southwesternmost and youngest volcano of this chain. It exhibits permanent degassing activity on its upper western and southern flanks. According to historic records it has been one of the most active volcanoes of the northern Chilean Andes during the nineteenth and twentieth centuries, with several small explosive eruptions which have generated thin tephra fallout deposits (Simkin & Siebert 1994). Guallatiri volcano consists essentially of a dome complex that has evolved in two main stages of middle to late Pleistocene and late Pleistocene to Holocene ages (García *et al.* 2004). It has generated a series of silicic andesite to dacite domes and their associated block-and-ash flow fans and tephra fallout deposits, with ages ranging from 710 to 5 ka. Block-and-ash flow fans are developed on its south and southwestern flanks, whereas the tephra fallout deposits are mainly located on the southern and eastern flanks of the volcano. A future eruption of Guallatiri could threaten the village of Guallatiri, located on its lower southern flank, and tephra could affect small villages in western Bolivia.

#### *Irruputuncu volcano (20.7°S, 68.6°W, 5163 m) (Fig. 5.5)*

This is located on the Chile–Bolivia border close to the large Collahuasi porphyry copper mine. Irruputuncu volcano shows permanent degassing activity, mainly through its central summit. The main gas released to the atmosphere corresponds to SO<sub>2</sub> (Clavero *et al.* 2005). Despite this permanent degassing, there are no reliable records of historical eruptive activity,



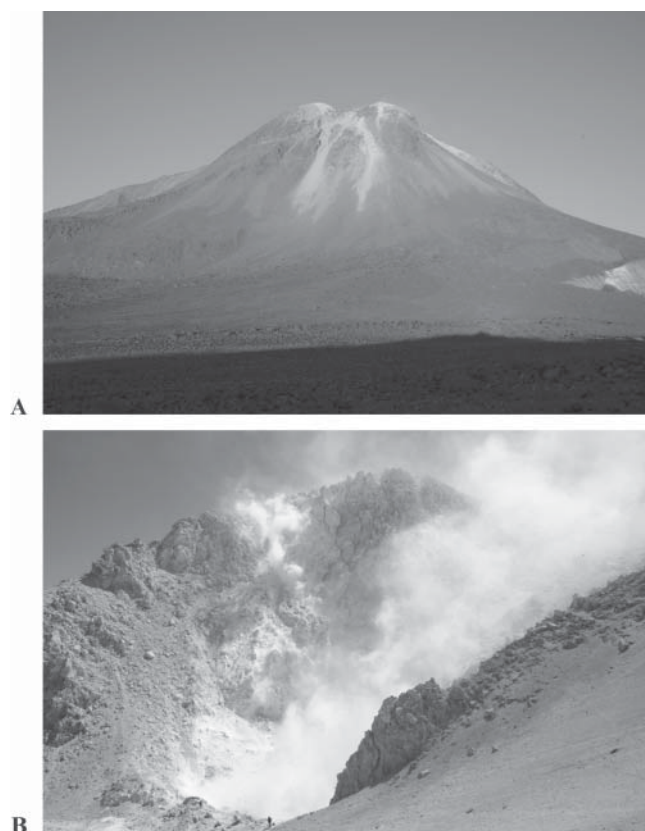


**Fig. 5.5.** (A) Irruputuncu volcano viewed from the SW. Photo by J. Clavero. (B) The active crater of Irruputuncu volcano from the NE, showing the intense degassing. Note person for scale in the lower central part. Photo by J. Lemp.

although unconfirmed press reports suggest a small eruptive event in 1989 (Simkin & Siebert 1994). Irruputuncu consists mainly of silicic andesite to dacite domes and lava-domes and their associated block-and-ash flow fans, especially developed towards the western and southern flanks. It has developed two craters, the southwestern one currently active. Wörner *et al.* (2000b) reported one reliable K–Ar age of a young dome on the upper western flank of c. 140 ka. Clavero (unpublished data) obtained a young  $1570 \pm 90$  years BP  $^{14}\text{C}$  date for a very fresh-looking block-and-ash flow deposit on the southwestern flank, demonstrating that Irruputuncu volcano has had explosive activity related to dome collapse in the Late Holocene. Although located in a very remote area, renewed activity could affect the main access road from Iquique to Collahuasi copper mine.

*Ollagüe volcano (21.3°S, 68.2°W, 5868 m) (Fig. 5.6)*

Located on the Chile–Bolivia border SW of the large Uyuni Salar, this volcano exhibits permanent fumaroles on its upper western and southern side, the latter being recently more active. The main gases are  $\text{SO}_2$  and  $\text{H}_2\text{O}$ , with minor fluxes of  $\text{CO}_2$  close to the fumarole vent (Clavero *et al.* 2005). Despite this fumarolic activity, there are no reliable records of historic eruptive activity, although unconfirmed reports suggest that an eruption may have occurred in 1903 (Simkin & Siebert 1994), and that an increase in fumarole ‘glowing’ may have occurred in November 2005 (A. Amigo and V. Sölar, pers. comm.). Ollagüe volcano is a long-lived stratovolcano, active since at least 1.2 Ma, that has produced rhyodacitic domes, silicic andesite lavas and domes, and dacitic domes and lava-domes, with their associated pyroclastic flow, surge and block-and-ash



**Fig. 5.6.** (A) Ollagüe volcano viewed from the NW, showing the main fumarole behind the post-avalanche upper dacite domes, and (B) from within the fumarolic crater on the south side, looking west over the debris avalanche deposit and La Poruña pyroclastic cone. Photos by J. Clavero.

flow deposits (Feeley *et al.* 1993; Feeley & Davidson 1994; Clavero *et al.* 2004c). The volcano has evolved mainly in three stages (Clavero *et al.* 2004c). Initially, at 0.9–1.2 Ma, a rhyodacitic dome complex formed along with its associated pyroclastic flow fan, including column-collapse pyroclastic flows and dome-collapse block-and-ash flows, which were directed mainly towards the northern and western flanks. It later evolved (600–900 ka) to a stratocone formed by andesitic to dacitic lavas, domes and associated block-and-ash flow deposits. During this stage the parasitic La Poruña pyroclastic cone was also erupted on the lower western flank of the volcano. At some point between 400 and 600 ka, a large sector collapse partially destroyed the ancestral edifice, generating a volcanic debris avalanche towards the west, covering a c. 50-km<sup>2</sup>-area of the Carcote Salar with an estimated debris volume of 1 km<sup>3</sup>, and involving salar deposits in the avalanche flow. Since the collapse (<400 ka), a series of dacitic domes and andesitic lavas have formed and partially filled the avalanche amphitheatre on the western flank of the volcano. Tephra fallout as well as block-and-ash-flow deposits have also been generated, the latter forming the youngest pyroclastic fan towards the lower western flank of the volcano.

*San Pedro (21.9°S, 68.4°W, 6145 m)*

This is a very large composite volcano, its peak rising 2500 m above its base. It forms the largest centre in a 16 km east–west volcanic lineament which also includes San Pablo volcano

(6092 m), an older, more eroded centre to the east, and, to the west, La Poruña pyroclastic cone and associated 8-km-long lava flow. San Pedro volcano shows almost permanent degassing activity on its upper central part. Simkin & Siebert (1994) report several eruptions within the nineteenth and twentieth centuries, although many of them are unconfirmed geologically.

San Pedro is formed by thick andesitic and dacitic lava flows and domes, with a smaller proportion of basaltic andesites (O'Callaghan & Francis 1986). The La Poruña lava flow is chemically similar to some of the volcanic units of San Pedro. San Pedro stratovolcano is formed by two separate stratocones, the older on the eastern side which collapsed to the west during an explosive eruption, generating a debris avalanche deposit associated with a pumice flow deposit (Francis *et al.* 1974). The amphitheatre generated by this collapse was filled by viscous lavas and pumice flows and block-and-ash flows, originally described as 'hot avalanche deposits' (Francis *et al.* 1974).

#### *Láscar volcano (23.4°S, 67.7°W, 5592 m)*

Located east of the Salar de Atacama, Láscar is the most active volcano of the northern Chilean Andes in historic times (Simkin & Siebert 1994), with more than 15 eruptive events of different magnitude in the twentieth century. The largest eruption (volcanic explosive index, VEI = 3–4) in the last 9000 years occurred in April 1993 (Fig. 5.7; Gardeweg *et al.* 1998b), when a subplinian eruptive column more than 20 km high rose above the crater, marking the end of an eruptive cycle that started in 1984 (Matthews *et al.* 1997). Small-volume pumice flows were formed when the column partially collapsed (Gardeweg & Lindsay 2004). These flows were directed towards the north-western and southern flanks of the volcano, reaching up to 9 km from their source (Guarinos & Guarinos 1993; Gardeweg & Medina 1994; Calder *et al.* 2000). The most recent eruption (before the time of writing: December 2005) of Láscar volcano occurred in May 2005 when a small explosion generated limited volumes of ash, which was dispersed towards northwestern Argentina. This event was not even noticed by the inhabitants of Talabre, the closest Chilean town to the volcano, 12 km to the west (Naranjo *et al.* 2006). The current activity of Láscar volcano consists of an almost permanent degassing through the active vent.

Láscar is a young, elongate, composite stratovolcano, with an estimated volume of 30–40 km<sup>3</sup>, active since 230 ka, whose structure is formed by two cones, on which five craters are developed, aligned in an ENE direction. Its eruptive activity has been divided into four stages (Gardeweg *et al.* 1998b). Stage I (230 to >26 ka; Gardeweg & Lindsay 2004) developed on an older stratocone formed mainly by andesitic lavas developed on



Fig. 5.7. April 1993 Subplinian (VEI = 3–4) eruption of the Láscar volcano. Photo courtesy of M. Gardeweg.

the eastern edge of the present edifice. This stage culminated with the eruption of andesitic pyroclastic flows. During Stage II (>26–22 ka) the magma composition changed to silicic andesite and dacite, and the eruptive activity migrated to the west, probably related to the formation of a dome complex. This stage ended with the Plinian eruption of a major ignimbrite: the Soncor ignimbrite (Gardeweg *et al.* 1998b; Matthews *et al.* 1999), which shows strong evidence for magma zonation, with juvenile material ranging from andesite to rhyodacite. A debris avalanche and the formation of a fluvio-glacial fan followed this large eruption between 22 and 19 ka. During Stage III (19.2–9.2 ka) a new stratocone was formed in the vent area of the Soncor eruption, consisting mainly of silicic andesite to dacite lavas, together with some andesitic pyroclastic flow deposits. This stage ended with a major explosive event, the Tumbres Eruption, which generated thin pumice fall deposits and a series of scoriaceous andesitic pyroclastic flow deposits. After the Tumbres event (Stage IV, 9.2 ka to the present) the activity shifted again to the east. Three aligned craters were formed and a series of thick lavas were erupted. The historical activity has been mainly characterized by periods of dome growth, crater subsidence and Vulcanian explosions. Since 1984, the activity has consisted of dome growth, crater subsidence, Vulcanian explosions and explosive eruptions, including the April 1993 Subplinian eruption, which generated small-volume pumice flow deposits.

Although located in a remote zone, far from populated areas, the 1993 eruption generated important effects in northwestern Argentina, demonstrating that the major hazard related to Chilean CVZ volcanoes corresponds to the effects of tephra dispersal reaching populated areas to the east in northwestern Argentina or southwestern Bolivia due to the predominant low-altitude wind direction in the Altiplano of northern Chile (Amigo & Gallardo 2004). However, larger eruptions could reach higher altitudes, where the wind direction changes, and tephra could be directed towards populated areas to the west in Chile (Amigo *et al.* 2006), as occurred several times between the Miocene and the Pleistocene in northern Chile (Basso *et al.* 2004).

#### *Socompa volcano (24.4°S, 68.3°W, 6051 m)*

Located along the Chile–Argentina border, this is a large stratovolcano without historical records of eruptive activity (de Silva & Francis 1991). Socompa volcano has mainly evolved in two stages, separated by a large sector collapse that affected the northwestern part of the edifice. The initial stratocone, which was higher than the current one, was formed mainly by andesitic to dacitic lavas, coulées, domes and subordinate pyroclastic flow and tephra fallout deposits (Déruelle 1978; Wadge *et al.* 1995). At c. 7,200 years BP (Francis & Wells 1988), a large volcanic debris avalanche, the largest known in the CVZ of the Andes, was formed, involving the partial collapse of the volcanic edifice and large volumes of its ductile basement (Francis *et al.* 1985; Wadge *et al.* 1995; van Wyk de Vries *et al.* 2001). The avalanche flow, directed towards the NW, travelled as far as 40 km from its source, inundating a total area of more than 500 km<sup>2</sup>, and generating a deposit with a minimum volume of 36 km<sup>3</sup> which was originally interpreted as the result of a 'nuée ardente' (Déruelle 1978). A pyroclastic flow, directed towards the NE, has been interpreted to have immediately followed the sector collapse (Francis *et al.* 1985). After this catastrophic event, a series of post-collapse domes, coulées and lavas, mainly dacitic in composition, partially filled the amphitheatre created by the collapse. A series of explosion craters within the collapse amphitheatre are likely to represent the most recent eruptive activity of Socompa volcano (Wadge *et al.* 1995).

#### *Llullaillaco volcano (24.7°S, 68.5°W, 6739 m)*

Located on the Chile–Argentina border, this is considered to be the second highest active volcano summit in the world.

Although it shows no signs of current fumarolic activity, there are records of at least three eruptions during the nineteenth century (Simkin & Siebert 1994). The evolution of Lullailaco volcano has been divided into two main stages according to geological mapping both in Chile (Gardeweg *et al.* 1984) and Argentina (Zapettini & Blasco 1998) and geochronological data (Richards & Villeneuve 2001). The first constructive stage (early Pleistocene) generated extensive dacitic lavas from two centres. These lavas have been strongly affected by hydrothermal alteration and glacial erosion. The second stage (late Pleistocene) generated a series of viscous dacite lavas, coulées and domes and associated block-and-ash flow deposits (de Silva & Francis 1991), forming a steep edifice built on top of the older eroded one. At some point during this late Pleistocene constructive phase (at *c.* 150 ka or later; Richards & Villeneuve 2001), a partial sector collapse affected the volcanic edifice, generating a large debris avalanche flow directed towards the east, which travelled for at least 25 km, resulting in a deposit that covers an area of *c.* 165 km<sup>2</sup> and has an estimated minimum volume of 1–2 km<sup>3</sup>.

*Lastarria (25.2°S, 68.5°W, 5697 m)*

This is a late Pleistocene to Holocene composite volcano which includes three morphostructural components: the Espolón Sur (Southern Spur), Lastarria volcano *sensu stricto*, whose activity has migrated northward with time along four seminested craters, and Negriales, a nearby 5.4 km<sup>3</sup> lava field (Naranjo 1988, 1992). Petrographically, the Lastarria complex consists of pyroxene andesites and pyroxene–amphibole dacites (Naranjo 1992). Lastarria has notably active fumaroles, but no reported record of historic eruptions. The stratigraphic succession suggests that the evolution of the volcanic complex started at Espolón Sur, and that Lastarria and Negriales evolved contemporaneously. No visible break occurs between the older and younger units. The modern Lastarria cone consists of well preserved lava flows and pyroclastic flows, including block-and-ash flows derived from the northernmost dome. A debris avalanche interpreted as a notably high-velocity flow was produced on the southeastern flank of the volcano after the collapse of the tephra-fall layers that form the entire upper part of the slightly concave slope of the cone (Naranjo & Francis 1987). In addition, 220–350-m-long sulphur flows, exhibiting well preserved pahoehoe structures, resulted from melting of hydrothermal sulphur deposits on the northwestern flanks of the cone due to enhanced thermal activity (Naranjo 1988).

*Nevado Ojos del Salado Volcanic Complex (27.1°S, 68.5°W, 6887 m)*

Located on the southern edge of the CVZ (Fig. 5.2), this is the highest active volcano summit in the world. It forms a volcanic group, together with the Pleistocene volcanic centres Nevado Tres Cruces, Volcán Solo, El Fraile and San Francisco (Gardeweg *et al.* 1997), oblique to the main chain of Pleistocene and Holocene CVZ volcanoes. Despite the fresh-looking aspect of the youngest lavas and domes, there are no reliable records of historical eruptive activity (Simkin & Siebert 1994), although unconfirmed reports by mountaineer guides suggest there was fumarolic activity in the 1980's (González-Ferrán *et al.* 1985). The Nevado Ojos del Salado volcanic complex corresponds to an extensive (*c.* 160 km<sup>2</sup>), long-lived field of andesitic, dacitic and minor rhyodacitic lavas, coulées and domes (Baker *et al.* 1987b; Gardeweg *et al.* 1997, 1998a) that has been active at least from early Pleistocene (*c.* 1.5 Ma, based on an age for a dacite lava of the lower northern flank) to late Pleistocene (*c.* 35 ka, based on the age for an upper dome of the northern flank) times, according to geochronological data (Gardeweg *et al.* 1997, 1999). This implies that its last eruptive activity was older than 30 ka. Despite the high silica content of most of the products of the Nevado Ojos del Salado volcanic complex, no

important pyroclastic deposits have been generated associated with this activity. The extensive pyroclastic cover of the volcano and its surroundings corresponds to a large explosive eruption of its neighbour Nevado Tres Cruces volcano, which occurred *c.* 67 ka ago.

*Nevado Tres Cruces volcano (27.1°S, 68.8°W, 6748 m)*

Located 20 km to the west of the Ojos del Salado volcanic complex, this eruptive centre also forms part of the oblique Pleistocene volcanic chain mentioned above. There are no records of historical activity, and so far the centre has not been listed as an active volcano (Simkin & Siebert 1994). Nevado Tres Cruces, which consists of at least three coalescent cones aligned in a north–south direction, is a long-lived stratovolcano, active since at least 1.5 Ma (Gardeweg *et al.* 2000). It is formed by a series of dacitic to rhyodacitic lavas, coulées, domes, explosive craters, and small-volume pyroclastic flow, surge and tephra fallout deposits (Gardeweg *et al.* 1997, 1999, 2000). It has produced at least two significant Pleistocene explosive eruptions, which have generated pyroclastic flows and tephra fallout deposits. The oldest of these explosive events took place at *c.* 1.5 Ma, generating a small-volume pyroclastic flow directed towards the west, whereas the youngest one took place at *c.* 67 ka, producing medium-volume pyroclastic flows, including 15-m-thick basal surge deposits, directed towards the east and SE. This eruption was associated with extensive tephra fallout deposits, which partially cover most of the surrounding areas towards the east, and were originally interpreted as being related to the Nevado Ojos del Salado volcanic complex (González-Ferrán *et al.* 1985). The youngest product of the volcano so far dated corresponds to a dacitic lava flow on its upper southern flank (*c.* 28 ka; Gardeweg *et al.* 2000), which implies volcanic activity in very late Pleistocene times.

## SVZ volcanoes of south-central Chile (H.M., L.L.-E., L.E.L., J.E.C., J.A.N. & C.R.S.)

Volcanoes of the Southern Volcanic Zone (SVZ; Figs 5.1 & 5.8) occur both in Chile and Argentina. In Chile alone, the SVZ includes > 70 Pleistocene and Holocene composite stratovolcanoes and large volcanic fields, and at least nine caldera complexes, as well as hundreds of minor eruptive centres (MEC) formed by scoria cones ± lava flows and maars. These form a continuous volcanic arc segment 1400 km long, extending from 33.3°S to 46°S. Between 33.3°S and 34.4°S the SVZ arc is a narrow chain of volcanoes located along the Chile–Argentina border, but between 34.4°S and 39.5°S the arc widens to > 200 km and occurs in both Chile and Argentina (Fig. 5.8). South of 39.5°S the SVZ again consists of a relatively narrow chain of volcanoes with the volcanic front in Chile, and south of 42°S all the arc volcanoes are located in Chile.

The SVZ has more historic volcanic activity, with about one eruption per year on average, than either of the other two volcanic zones in Chile. Villarrica and Llaima volcanoes are two of the most active volcanoes in the entire Andean arc, with together more than 80 reported episodes of activity since 1558 (Simkin & Siebert 1994; Petit-Breuilh 1994; Petit-Breuilh & Lobato 1994; Naranjo & Moreno 2005). The largest historic eruption (*c.* 9.5 km<sup>3</sup>) of any Chilean volcano, and the largest of any Andean volcano in the last 100 years, was generated by Quizapu in 1932 (Hildreth & Drake 1992). Among the > 70 stratovolcano complexes and volcanic fields between 33.3°S and 46°S, at least 40 have erupted in the Holocene and 20 have had historic eruptions. Most of the hundreds of MEC cones and maars are also Holocene, and three of them (Riñinahue, Carrán and Mirador) erupted during the last century. Six of the nine calderas have erupted in the past < 1 Ma. Large volumes of middle Pleistocene rhyolite pyroclastic flows derived from the Diamante and Calabozos calderas (Fig. 5.8; Stern *et al.*



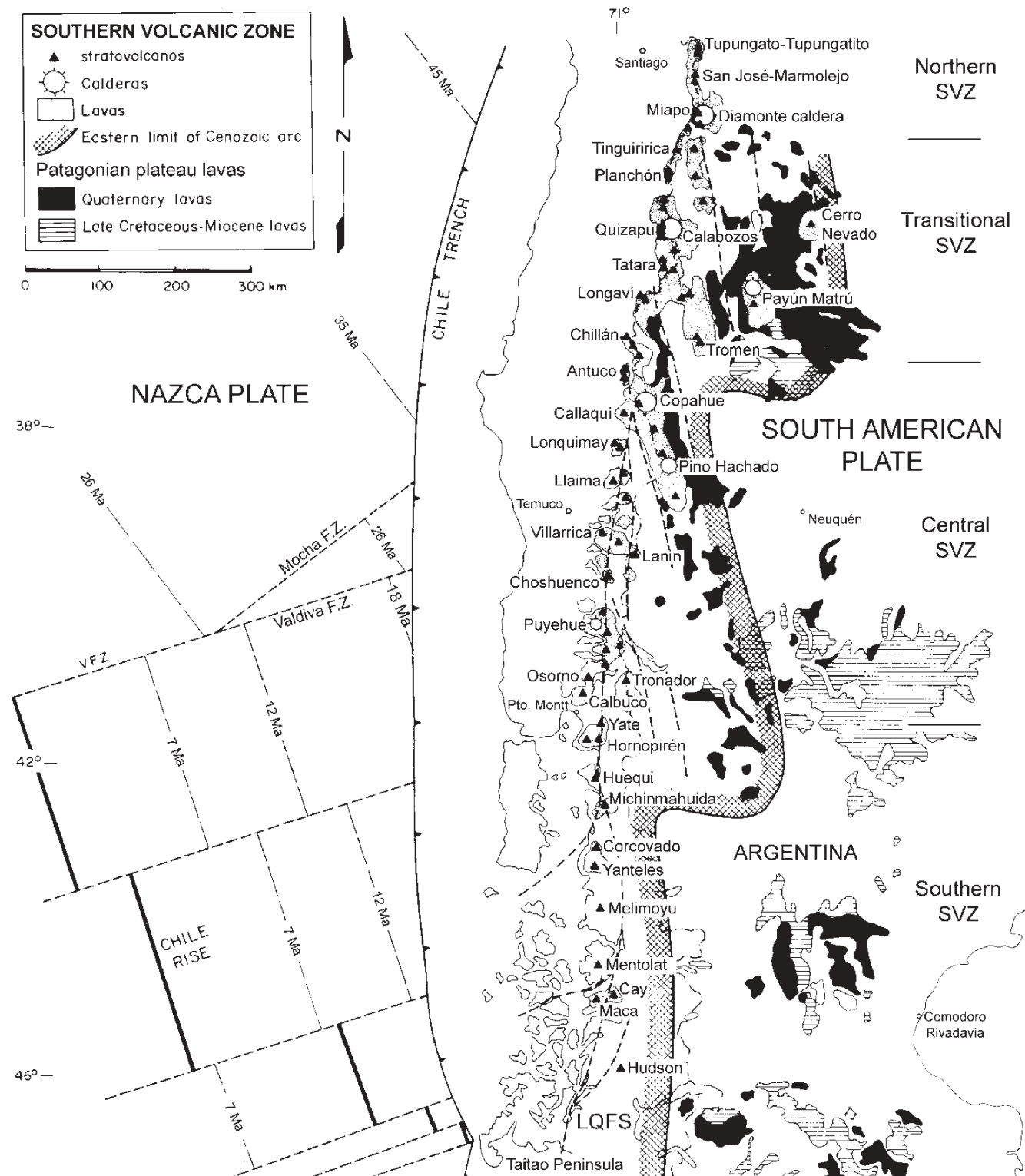


Fig. 5.8. Schematic map of the location of some of the volcanoes and larger caldera systems in the Southern Volcanic Zone. Dark cross-hatched line indicates the eastern limit of Cenozoic arc volcanism, which divides the area of transitional (to the west) from cratonic (to the east) alkali olivine backarc basalts of the Patagonian plateau lavas (Stern *et al.* 1990). The approximately north-south dashed line labelled LOFS is the Liquiñe-Ofqui Fault System.

1984a; Hildreth *et al.* 1984) have travelled more than 100 km from their sources in the High Andes and crossed the Central Valley between Santiago and Puerto Montt where the largest part of the population of Chile lives. Although such large eruptions are infrequent, Hildreth *et al.* (1984) noted that the 'long record of voluminous silicic pyroclastic activity' associated with

these giant systems 'has important implications for the safety of several major cities near the mouths of Andean canyons'. Smaller, but still aerially extensive pyroclastic flows, derived from explosive eruptions of other SVZ volcanoes, as well as lahars and debris flows, have also covered what are today highly populated regions of the Central Valley.

### Geological and tectonic setting

The Southern Volcanic Zone (SVZ) of central-south Chile results from the subduction of the oceanic Nazca Plate under the South American Plate (Figs 5.1 & 5.8). Its northern end coincides with the impingement of the Juan Fernández Ridge (JFR) upon the Chile–Peru trench, which is accompanied by a dramatic change in the subduction angle of the Nazca Plate below South America (Fig. 5.1). The southern boundary of the SVZ is the intersection of the Chile Ridge with the trench. Convergence direction between the Nazca and South American plates is oblique (*c.* 20–30°; Jarrard 1986; Dewey & Lamb 1992) and convergence velocity is 7–9 cm/year (DeMets *et al.* 1990). The age of the Nazca Plate at the trench decreases from 45 Ma in the north to 0 Ma at the southern end of the SVZ. Subduction angle increases from *c.* 20° at the northern end of the SVZ to >25° further south. As a consequence, the distance from the trench to the volcanic front decreases from >290 km in the north to <270 km in the south. In part because of the change in the distance of the volcanic front from the trench, the volcanoes along the front at the northern end of the SVZ occur in the High Andes along the drainage divide between Chile and Argentina, while to the south they occur in Chile along the western margin of the Andean Cordillera with the Central Valley, an extensional basin formed at the beginning of late Oligocene times (Muñoz *et al.* 2000). Crustal thickness also decreases from 55–60 km at the northern end of the SVZ to <35 km south of 37°S. The crust below the SVZ consists of Palaeozoic and Mesozoic pre-Andean basement and Mesozoic–Cenozoic igneous rocks.

In southern Chile (39–47°S), oblique convergence results in slip along the arc-parallel Liquiñe–Ofqui Fault System (LOFS in Fig. 5.8; Cembrano *et al.* 1996, 2000; Lavenu & Cembrano 1999a, b; Arancibia *et al.* 1999). This fault system controls the location of many of the larger volcanic centres as well as MEC monogenetic cones in the southern SVZ (López-Escobar *et al.* 1995a). In contrast, in northern and central Chile (20–34°S), crustal shortening occurs with only minor arc-parallel slip (Dewey & Lamb 1992). A transitional zone between these two areas occurs in central-south Chile (34–39°S), where the SVZ is widest and includes extensional intra-arc basins with small monogenetic basaltic cones and alkali basalt lava fields (Fig. 5.8; Muñoz & Stern 1988, 1989; Folguera *et al.* 2002). In this part of the arc the location of stratovolcanoes and calderas is controlled chiefly by NW–SE and NE–SW structures.

### SVZ volcanoes and volcanic hazards

Post-glacial eruptions of SVZ volcanoes include the full range of Hawaiian, Strombolian, Subplinian, Plinian, Vulcanian and phreatomagmatic types, with VEI (Newhall & Self 1982) ranging from 0 to 6. There appears to be a relation between magma composition and eruption style. Basaltic to basaltic andesitic magmas have had mainly Strombolian eruptions, which normally can also include Hawaiian phases, such as the typical historic eruptions of Antuco, Llaima, Villarrica and Osorno. High-silica andesitic and dacitic magmas commonly have had Subplinian eruptions, as for example the historic eruptions of Descabezado Grande (1932), Cordón Caulle (1922 and 1960) and Calbuco (1961). High-silica dacites to rhyolitic magmas have had Subplinian and Plinian eruptions, such as the eruptions of Quizapu in 1932 and Hudson in 1991. Important exceptions are the pre-historic eruptions of the 24 km<sup>3</sup> basaltic to basaltic andesite Curacautín Ignimbrite from the Llaima volcano at *c.* 13.5 ka (Naranjo & Moreno 1991), and the *c.* 6.7 ka Hudson explosive eruption of >18 km<sup>3</sup> of low-silica andesite (Stern 1991d; Naranjo & Stern 1998).

Lahars, lava flows and ashfalls have been the main volcanic hazards within historic times. Lahars produced by the eruptions of Villarrica volcano in 1948–49, 1963–64 and 1971–72 together killed more than 75 people (Lara & Clavero 2004). A giant lahar generated in 1971 by melting of glacial ice in the

Hudson caldera flowed over 40 km from its source to the sea (Best 1992). Lahars may also be generated by lava flows temporarily obstructing drainage systems. Ashfall produced by both the 1932 eruption of Quizapu and the 1991 eruption of Hudson adversely affected very large regions to the east in Argentina. Ashfall produced by explosive eruptions in the SVZ has the potential to significantly disrupt both domestic and international air traffic across the southern part of South America (Hauser & Naranjo 2006).

Pyroclastic flows and surges, together with voluminous debris avalanches, have also occurred during latest Pleistocene and Holocene times. Three late Pleistocene large-volume pyroclastic flows have crossed the Central Valley between Santiago and Puerto Montt, travelling more than 100 km from their sources. Lateral blasts followed by small surges took place in the 1864 eruption of Mocho-Choshuenco, and the 1893–95 and 1929 eruptions of Calbuco volcanoes. San Pedro, Antuco and Calbuco had Bezimmiany- and Bandai-types cone sector collapses between 14000 and 6200 years BP, generating large debris avalanches (6–15 km<sup>3</sup>).

On the basis of the tectonic controls affecting the distribution of volcanic centres, as well as petrologic and geochemical considerations, the Pleistocene and Holocene volcanoes of the SVZ are divided into four main provinces or segments (Fig. 5.8; Tormey *et al.* 1991a; López-Escobar *et al.* 1995a; Stern 2004). These are the Northern (NSVZ; 33.3–34.4°S), Transitional (TSVZ; 34.4–37°S), Central (CSVZ; 37–42°S) and Southern (SSVZ; 42–46°S) segments. Volcanoes and volcanic hazards for each of these provinces are discussed separately below.

### The NSVZ

The NSVZ is formed by eight composite stratovolcanoes and the giant Diamante caldera, aligned in a north–south trend along the High Andes drainage divide between Chile and Argentina (Fig. 5.8). An older early to mid-Pleistocene volcanic chain forms the base for younger late Pleistocene to Holocene volcanoes. The volcanic front in the Pliocene was further to the west, but migrated to its current position as a result of both decreasing subduction angle and subduction erosion below the northern end of the SVZ (Stern 1989, 1991b; Kay *et al.* 2005), possibly due to the southward migration of the locus of subduction of the Juan Fernández Ridge (Fig. 5.1; Stern & Skewes 1995, 2005; Yañez *et al.* 2001, 2002).

Summit elevations of volcano edifices in the NSVZ are <2000 m above their base, and basal elevations decrease in height from north to south. Thus Tupungato volcano (6570 m), the northernmost and highest volcano in the SVZ, has its base over Mesozoic strata at 4600 m, while the Maipo volcano (5290 m), the southernmost in the NSVZ, located inside the Diamante caldera (Fig. 5.9), overlies basement with an average elevation of 3600 m. The Diamante caldera erupted an estimated 450 km<sup>3</sup> of rhyolite pyroclastic material in the middle Pleistocene (Stern *et al.* 1984a). The largest stratovolcano in the region is the lower to middle Pleistocene Marmolejo centre (Fig. 5.10), but the volumes of other NSVZ volcanoes are relatively small, from 5 to 55 km<sup>3</sup> (Hildreth & Moorbath 1988). This reflects a relatively low rate of magma extrusion from the stratovolcanoes in the NSVZ during the late Pleistocene and Holocene (Stern *et al.* 1984a).

From north to south in the NSVZ, the older group of centres includes the Nevado de Piuquenes (6019 m) and Marmolejo (6108 m; López-Escobar *et al.* 1985) centres, and further south the isolated Castillo (5485 m) centre, the 15 × 20 km wide Diamante caldera (Stern *et al.* 1984a; Ruoga *et al.* 2005), Listado (4250 m) and Picos del Barroso (5000 m). All are deeply eroded and the northernmost ones collapsed laterally, forming non-volcanic debris avalanches, due to instability caused by both hydrothermal alteration and strong erosion. The younger group consists of well-preserved stratocones like Tupungato, the Tupungatito craters cluster (5682 m),



**Fig. 5.9.** Maipo volcano and Diamante lake viewed from the east inside the Diamante caldera. Photo by C.R. Stern.



**Fig. 5.10.** Marmolejo volcano, the largest in the NSVZ, and San José unglaciated Holocene cone above eroded Marmolejo lavas on the right, looking towards the east along the valley of the Volcán river. Photo by C.R. Stern.

the San José volcanic complex (5856 m) overlying Marmolejo (Fig. 5.10), and Maipo volcano inside the Diamante caldera (Fig. 5.9).

Among these volcanoes, Tupungatito, San José and Maipo have had historic eruptions, most recently in 1987, 1960 and 1912, respectively, and both Tupungatito and San José show permanent solfataric activity. These three historically active volcanic centres all have high summit elevations ( $>5290$  m), are snow- and ice-covered, and occur at the source of relatively narrow mountain drainage systems that ultimately feed into the Maipo River, which flows through the southern edge of Santiago, the largest city in Chile. Thus, although these centres are not visible from Santiago, and are located relatively far from the city, they pose a potential sector-collapse, debris-flow hazard to the  $>6\,000\,000$  inhabitants of the city, as well as tephra-fall hazard that might impact the Province of Mendoza to the east in Argentina and disturb air traffic in both countries.

Rhyolite pyroclastic material from the middle Pleistocene eruption that formed the giant Diamante caldera flowed into the area of the northern Central Valley now occupied by the cities of Santiago and Rancagua, forming the  $>30$ -m-thick Pudahuel ignimbrite, as well as out to the east onto the plains south of Mendoza, Argentina (Stern *et al.* 1984a). However, such very large eruptions are extremely infrequent, and no such giant eruption has occurred anywhere in the Andes during Holocene times.

### *The TSVZ*

From  $34.4^{\circ}\text{S}$  to  $37.0^{\circ}\text{S}$ , the Pleistocene and Holocene volcanic front trends  $\text{N}20^{\circ}\text{E}$ . The arc also widens considerably eastward into Argentina (Fig. 5.8), with arc volcanic centres located along NW–SE trending uplifted blocks separated by intra-arc extensional basins containing small basaltic cones and lava flows (Muñoz & Stern 1988, 1989). Within the arc, transverse alignments control the location of several volcanic vents south of the Planchón–Peteroa–Azufre volcanic complex. Thus, Descabezado Chico and the San Pedro–Tatara–Pellado volcanic complexes are arranged along a NE–SW alignment and a NW–SE trend controls both the Nevado de Longaví–Loma Seca–Resago volcanoes and the Nevados de Chillán volcanic complex.

The TSVZ is characterized by compound stratovolcanoes and large volcanic complexes that overlie older basaltic shield volcanoes, as well as volcanic fields and giant calderas. Most of the latter are related to late Pliocene to Pleistocene volcanic activity. The heights of the volcanic edifices in the TSVZ are  $<1900$  m above their bases, and most of them are only between 1400 and 1700 m. Their volumes are relatively small, from 3 to  $60\text{ km}^3$  (Hildreth & Moorbath 1988), but some of the caldera systems have erupted large volumes of Pleistocene rhyolites (Hildreth *et al.* 1984, 1999). Basal elevations along the volcanic front decrease from north to south, both because the Andes are not as high towards the south, and also because the location of the volcanic front moves westward from along the drainage divide between Chile and Argentina towards the western edge of the Cordillera (Hildreth & Moorbath 1988). Thus the small Palomo volcano (4850 m) overlies Mesozoic and Cenozoic rocks that have a height of about 3400 m, while the larger Nevados de Chillán volcanic complex (3216 m) overlies a basement with an average height of only 1500 m. Numerous small cities and rural population centres in the Central Valley occur along rivers that have their origin on the flanks of large TSVZ volcanoes.

From north to south, the 12 most important middle-late Pleistocene to Holocene TSVZ volcanic centres and volcanic fields in Chile are Palomo (4850 m), the Tinguiririca cluster (Arcos *et al.* 1988), Planchón–Peteroa–Azufre (Tormey *et al.* 1995; Naranjo *et al.* 1999a; Naranjo & Haller 2002), the Descabezado Grande–Quizapu–Azul volcanic complex (Hildreth & Drake 1992), the Descabezado Chico volcanic complex (3250 m), the Calabozos caldera (Hildreth *et al.* 1984), the Del Medio volcanic complex (3508 m), the San Pedro–Tatara–Pellado volcanic complex (Dungan *et al.* 2001), the Laguna del Maule volcanic field (3175 m; Frey *et al.* 1984; Hildreth *et al.* 2004), which has a longer history that began in Pliocene times, the Nevado de Longaví (3242 m; Sellés *et al.* 2004), Loma Blanca (2230 m), Resago (1890 m) and the Nevado de Chillán volcanic complex (Dixon *et al.*, 1999; Naranjo and Lara, 2004). Older highly eroded stratovolcanoes and calderas, probably of lower to middle Pleistocene age, include the western margin of the giant  $35 \times 45$  km wide Del Atuel caldera, Alto del Padre–Sordo Lucas (3548 m) and Campanario (4020 m; Hildreth *et al.* 1998).

The largest volcanic areas in the TSVZ of Chile are the ones formed by the Descabezados, Calabozos and Laguna del Maule volcanic fields, which together contain more than 200 vents, including stratovolcanoes, craters, scoria cones, domes and maars. The main historically active and potentially hazardous volcanic complexes, each summarized briefly below, are Tinguiririca, Planchón, Descabezado Grande–Quizapu–Azul, San Pedro–Tatara–Pellado and Nevados de Chillán.

**Tinguiririca ( $34.8^{\circ}\text{S}$ ,  $70.3^{\circ}\text{W}$ , 4300 m).** This is a Holocene cluster of about ten scoria cones, the southernmost one called Fray Carlos. The cluster overlies a lower to middle Pleistocene plateau of andesitic lavas (Arcos *et al.* 1988). The last eruption was in 1917 and this centre has permanent solfataric activity.





N140°E (Dixon *et al.* 1999). Early eruptive activity is represented by a succession of extensive pyroclastic flow deposits and remnants of a caldera structure, probably of late Pleistocene age (Dixon *et al.* 1999). The two subcomplexes are late Pleistocene to Holocene in age (<30 ka) and have evolved contemporaneously but with different magmatic signatures (Dixon *et al.* 1999). The Cerro Blanco subcomplex (3212 m) consists of an early shield volcano, followed by the construction of a stratocone, with andesite to dacite lavas. The latter, formed by a series of overlapping cones, had a sector collapse and suffered glacial erosion. The youngest cones contain pyroclastic ejecta and lavas with silicic dacite or andesite compositions. The Las Termas subcomplex can be divided into a pre-caldera sequence, formed essentially by andesite lavas, and a late Pleistocene post-caldera sequence also formed by andesite lavas, some of them reaching up to 35 km from their source (Naranjo *et al.* 1994a). Various overlapping cones and explosive craters, developed beginning in the late Pleistocene, have generated several Holocene Subplinian and Vulcanian eruptions. The historically active cones and craters, which include Arrau, Nuevo and Chillán volcanoes, belong to the Las Termas subcomplex (Dixon *et al.* 1999). Nuevo volcano was formed during the long-lasting eruption of 1906–45, and Arrau volcano was formed during the 1973–86 eruptive event. The most recent small-volume explosive eruption of the Nevados de Chillán complex occurred in 2003 (Naranjo & Lara 2004).

Based on historic activity, the main hazards related to Chillán volcano correspond to the generation of lavas, parasitic pyroclastic cones with associated tephra fallout and minor lahars. However, Nevados de Chillán has generated large Pleistocene ignimbrites that have crossed the Central Valley (Dixon *et al.* 1999). Viejo cone (3112 m) has been the source of several moderate-magnitude Subplinian and Vulcanian explosive eruptions during Holocene times, but these produced only small pyroclastic flows along with tephra falls. In 1861 the Santa Gertrudis cone subglacial eruption produced a lahar along the Ñuble river that destroyed many houses and bridges as far as 80 km downstream and ultimately reached the Central Valley, although in general Chillán has not generated large lahars.

### The CSVZ

The northern sector of the CSVZ (37–39°S), like the TSVZ, is a broad arc up to 120 km wide, with intra-arc basins and arc volcanoes in Argentina (Fig. 5.8; Muñoz & Stern 1988, 1989). South of 39°S, the CSVZ narrows into a chain only about 80 km wide without intra-arc basins. The volcanic front of the CSVZ occurs west of the drainage divide between Chile and Argentina. The volcanic front of the CSVZ either migrated west to its current position in the late Pleistocene (Stern 1989), or the amplitude of volcanic activity along the current front increased significantly at this time (Lara *et al.* 2001; Mella *et al.* 2005; Lara & Folguera 2006). The front consists of middle to late Pleistocene to Holocene stratovolcanoes that overlie deeply eroded Pliocene and Pleistocene volcanic edifices. South of 40.5°S the modern stratovolcanoes occur along the western margin of the Main Cordillera.

South of 38°S, the arc-parallel Liquiñe–Ofqui Fault System (LOFS in Fig. 5.8) controls the location of many of the larger volcanic centres as well as MEC monogenic cones in CSVZ (López-Escobar *et al.* 1995a). Although the volcanic arc has an almost north-south trend, oblique alignments control the location of many of the volcanic complexes and large stratovolcanoes along prevailing NW–SE and NE–SW directions. SVZ volcano edifices reach their maximum size in the CSVZ, rising up to 2600 m above their base, covering more than 500 km<sup>2</sup> and reaching volumes of hundreds of cubic kilometres. Basal elevations decrease in height from north to south. The northernmost Antuco (2979 m)–Sierra Velluda (3585 m) volcanic complex has developed over Cenozoic sedimentary and granitic rocks that are about 1350 m high, while the southern Osorno volcano (2652 m) overlies a similar basement, but with an average elevation of only 150 m.

The CSVZ Late Pleistocene to Holocene volcanic front includes, from north to south, the following centres: Antuco (López-Escobar *et al.* 1981), Callaqui (Polanco 1998), Tolguaca (2806 m; Polanco 1998), Lonquimay (2865 m; Moreno & Gardeweg 1989; Naranjo *et al.* 1992), Llaima (Naranjo & Moreno 1991, 2005; Moreno & Naranjo 2003), Solipulli caldera (2282 m; Naranjo *et al.* 1993a; Gilbert *et al.* 1996), Caburgua cluster (998 m), Villarrica (Clavero & Moreno 1994, 2004; Petit-Breuilh 1994; Moreno 2000; Lara & Clavero 2004), Mocho–Choshuenco complex (Echegaray 2004), Carrán–Los Venados cluster (Campos *et al.* 1998; Lara *et al.* 2006b), Cordillera Nevada caldera (1799 m), Cordon Caulle fissural range (Lara *et al.* 2004b, 2006a, b) and Puyehue caldera (Gerlach *et al.* 1988), Antillanca (or Casablanca) cluster (1990 m), Cenizos (1668 m), Osorno (López-Escobar *et al.* 1992) and Calbuco (Hickey-Vargas *et al.* 1995; López-Escobar *et al.* 1995b). Among them are lower and/or middle Pleistocene eroded stratovolcanoes such as Sierra Velluda (3585 m), Lancú (2296 m), Sierra Nevada (2554 m), Llalliqupe (1915 m), Quinquilil (2002 m), Quinchilca caldera (1632 m), Mencheca (1840 m), Sarnoso (1630 m), La Picada (1715 m) and Hueñuhueñu (1207 m).

Between 38°S and 39.5°S, the eastern part of the arc in Chile includes the middle Pleistocene to Holocene Copahue stratovolcano (Fig. 5.12; Varekamp *et al.* 2001; Polanco 2003; Naranjo & Polanco 2004) located on the western edge of the giant El Agrio (or Caviahué) caldera (Muñoz & Stern 1988, 1989; Folguera & Ramos 2000; Melnick & Folguera 2001; Melnick *et al.* 2006). Southeast of Copahue, small Holocene scoria cones and maars overlie a Pliocene and Pleistocene volcanic plateau and old eroded stratovolcanoes that include the Lower Pleistocene Pino Hachado caldera (Fig. 5.12; Muñoz & Stern 1988, 1989; Tunstall & Ramos 2005). Behind the volcanic front south of 39.5°S, volcanic centres are mostly eroded lower to middle Pleistocene stratovolcanoes, but a few are late Pleistocene to Holocene stratocones. These include, from north to south, Quetripillán complex (Pavez 1997; Pavez *et al.* 2004), Lanín (Fig. 5.13; Lara & Moreno 1994b; Lara *et al.* 2004a), Huanquihue complex (2139 m), Chihuío (Lara and Moreno 2004; Lara & Folguera 2006), Pirehueico (Lara & Moreno 2004; Lara & Folguera 2006), Mirador (1795 m), Pantoja (2024 m), Puntagudo (2493 m), Tronador (3491 m; Mella *et al.* 2005), Cerro Volcánico (1930 m) and Cuernos del Diablo (1862 m).

This CSVZ is the most volcanically active segment along the whole Andes and includes two of the most active volcanoes in South America: Llaima and Villarrica. Llaima, Villarrica and Tronador are the largest individual volcanoes in the CSVZ, with volumes up to >400 km<sup>3</sup>. Growth rates of 4 km<sup>3</sup> in less than 10000 years have been determined for Antuco volcano. The largest volcanic fields in the CSVZ are the ones formed by the Cordillera Nevada caldera, Cordon Caulle fissural range, Puyehue, Mencheca and Carrán–Los Venados clusters that together cover an area of more than 1500 km<sup>2</sup>, with almost 200 vents including stratovolcanoes, calderas, craters, scoria cones, domes, fissures and maars. Numerous minor eruptive centres such as Rucapillán, Caburgua, La Barda, Redondo, Relicura, Huelemolle, Riñinahue, Carrán and Mirador, among many others, also occur in the vicinity of the larger stratovolcanoes and along the LOFS (López-Escobar *et al.* 1995a).

The numerous historically active volcanoes, their large size and proximity to the eastern edge of the Central Valley make the CSVZ an area of high volcanic risk. Risk has been enhanced in this region by the construction of dams along drainages originating on the flanks of volcanoes. In 1996 the Servicio Nacional de Geología y Minería (SERNAGEOMIN) created the Observatorio Volcanológico de los Andes del Sur (OVDAS) in Temuco to monitor the more hazardous volcanoes along the SVZ, particularly Llaima and Villarrica volcanoes. Currently, Lonquimay, Mocho–Choshuenco,



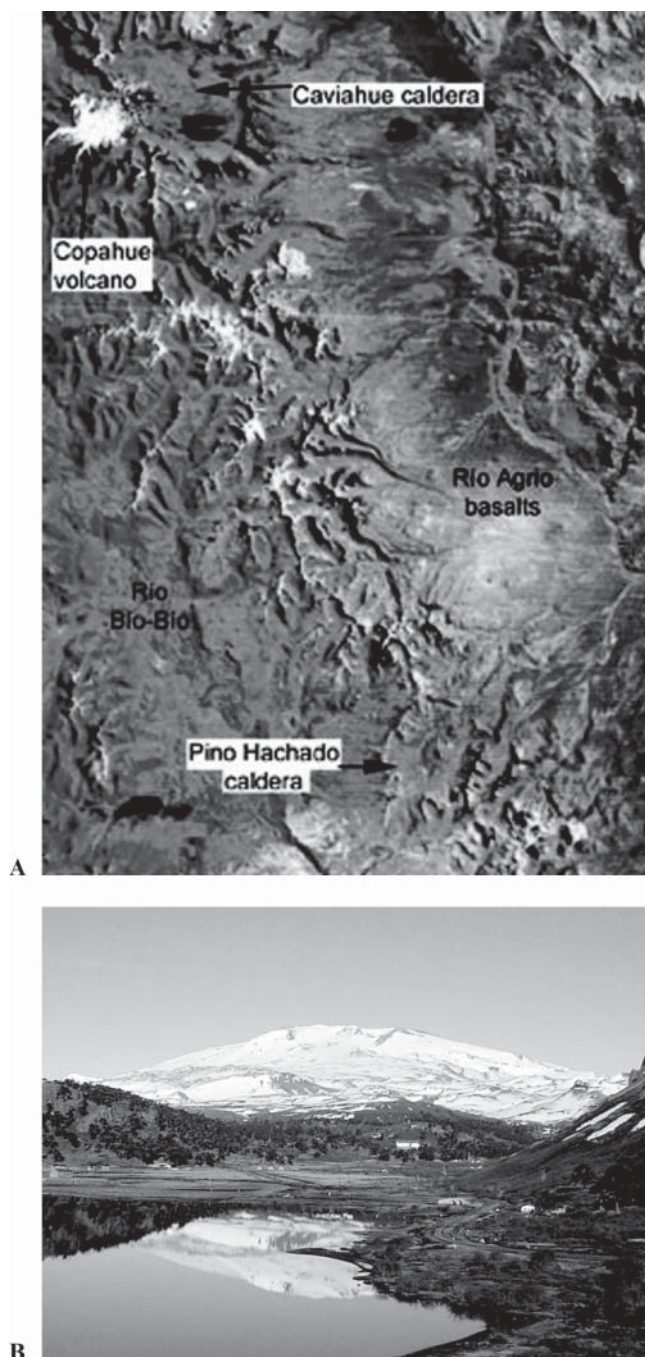


**Fig. 5.12.** (A) Satellite photo of Copahue volcano inside the Agrio (Caviahue) caldera at the northwestern end of the NW–SE chain of Pliocene and early Pleistocene volcanic centres which include the Pino Hachado caldera. (B) Photo (by J. Clavero) of the Copahue volcano viewed from the east.

Osorno and Calbuco volcanoes are also seismically monitored through OVDAS.

The historically most active and potentially most hazardous CSVZ volcanic complexes, briefly described below, include Antuco, Callaqui, Copahue, Lonquimay, Llaima, Villarrica, Quetrupillán, Carrán–Los Venados, Puyehue–Cordón Caulle fissural range, Osorno and Calbuco.

**Antuco (37.4°S, 71.4°W, 2979 m).** This is a compound stratovolcano, active since late Pleistocene times, which overlaps the larger eroded Sierra Velluda stratovolcano (3385 m). An early



**Fig. 5.13.** Lanín volcano viewed from the north. Photo by L.E. Lara.

edifice collapsed laterally to the west after a 6.2 ka Bandai-type eruption, leaving a 2-km-wide horse-shoe-shaped crater and generating a  $> 5 \text{ km}^3$  debris avalanche that reached the Central Valley. The current stratocone grew inside the avalanche crater. Antuco has had at least 17 historic eruptions, with the last big eruption occurring in 1853 and the last recorded event being in 1911. Currently it has weak fumarolic activity on the summit.

**Callaqui stratovolcano (37.9°S, 71.4°W, 3100 m).** This eruptive centre is strongly controlled by a NE–SW fissure with an 11-km-long row of craters and a main summit crater filled with ice. It is a dominantly basaltic–andesite to andesite volcano and has been active since the Late Pleistocene. At least five historic eruptions have been recorded for this volcano. The last was a small event that took place in 1980. Currently it has strong solfataric activity on the south flank near the summit. Based on morphostructural features and both K–Ar and  $^{14}\text{C}$  dates, six chronostratigraphic units, with ages ranging from 171 ka to Holocene, have been mapped (Naranjo *et al.* 1999b). Small-volume pyroclastic flow deposits have been dated between 9950 and 320 BP. One of the most important hazards associated with Callaqui volcano is the generation of large lahar flows that are widely distributed in the surrounding drainages.

**Copahue volcano (37.8°S, 71.2°W, 2965 m).** This is a Pleistocene to Holocene stratovolcano, built on the southwestern edge of the Pliocene El Agrio (or Caviahue) caldera (Fig. 5.12; Muñoz & Stern 1989; Pesce 1989; Linares *et al.* 1999; Folguera & Ramos 2000; Melnick & Folguera 2001; Melnick *et al.* 2006). Copahue volcano has an elongated shape (22 km  $\times$  8 km), with nine summit craters aligned at N60°E. The easternmost crater (2800 m) is currently active. Since its earlier stages at *c.* 1.2 Ma (Polanco 2003), Copahue has produced mainly andesite to basaltic andesite lavas, although subordinate rhyolite domes and pyroclastic deposits also occur. Holocene explosive eruptions have generated several pyroclastic deposits (*c.* 8–2 ka BP), including pyroclastic flow, surge and tephra fallout (Polanco 1998, 2003; Polanco *et al.* 2000). There are records of at least 12 eruptive events in the last 250 years, most of them of phreatic origin (Petit-Breuilh 1996; Martini *et al.* 1997). One of the best-documented eruptions took place between July and August 1992, when both phreatic and phreatomagmatic explosions occurred (Delpino & Bermúdez 1993). The last important eruption of Copahue volcano took place from July to October 2000 (Naranjo & Polanco 2004). The main volcanic hazards related to a future eruption of Copahue volcano are the generation of pyroclastic flows, tephra fallout, lavas and lahars (Delpino & Bermúdez 1994; Naranjo *et al.* 2000a). However, the presence of an acid lake within the active crater (Varekamp *et al.* 2001) represents one of the most hazardous aspects that could threaten Caviahue, the closest village to the volcano.





**Fig. 5.14.** The 1988–89 eruption of Navidad cone flanking the Longuimay volcano. Photo by H. Moreno.

**Longuimay volcano (38.3°S; 71.5°W, 2865 m) (Fig. 5.14).** This is a stratovolcano that has been active mainly in Holocene times (Moreno & Gardeweg 1989). It has a truncated cone due to an ENE fracture control and an estimated edifice volume of *c.* 20 km<sup>3</sup>. Its eruptive activity has been divided into six lava units, including the most recent eruptive products generated in the 1988–89 eruption. Lavas are andesite to basaltic andesite in composition and vary from aa to blocky in morphology, with minor basalts and dacites. A succession of pyroclastic deposits, which include both pyroclastic flow and tephra fallout, have been recognized. Although they correspond to small-volume eruptions (Strombolian to Subplinian), some pyroclastic flows reached areas located more than 10 km from their source, with the last of these being erupted only *c.* 200 years ago (Naranjo *et al.* 2000*a, b*). There are no reliable records of historic eruptions occurring through the main vent. Instead, seven documented eruptive events have been attributed to flank eruptions, including the last long-lasting eruption of 1988–89. This eruption generated a flank pyroclastic cone (Navidad cone; Fig. 5.14) and an associated lava flow (Moreno & Gardeweg 1989; Gardeweg *et al.* 1990; Naranjo *et al.* 1992). The maximum eruptive column height was estimated at 9 km above the vent with an estimated VEI of 1–2, and the lava flow reached up to 10.2 km from the source. The high fluorine content produced widespread pollution of land, air and water which strongly affected both humans and grazing animals. According to the historical and post-glacial activity, the main hazards related to Longuimay volcano are the formation of new flank vents, the emission of volcanic products with high fluorine content and the consequent contamination of water, grass and atmosphere, and tephra fallout (Naranjo *et al.* 2000*a, b*). Another important hazard, although less recurrent, is small-volume pyroclastic flows, which can reach populated areas.

**Llaima volcano (38.6°S, 71.6°W, 3179 m) (Fig. 5.15).** This is one of the most historically active volcanoes in the entire Andean chain, with more than 49 reported eruptions since 1640 (Petit-Breuilh & Lobato 1994; Naranjo & Moreno 2005). It is a large compound stratovolcano, one of the largest in the Chilean Andes (up to 400 km<sup>3</sup> in volume), whose products cover an area of more than 500 km<sup>2</sup>. It consists of a composite stratocone that developed on the eastern side of a NE fissural range, both built on top of an older shield volcano formed by a lava succession erupted from the central and flank vents. The evolution of Llaima volcano has been divided into three main stages (Naranjo & Moreno 2005). During its early stage it generated a shield-like volcano mainly formed by basaltic andesite lavas, with minor basaltic andesites, subsequently glacially eroded



**Fig. 5.15.** (A) Llaima volcano, one of the largest in the SVZ, viewed from the west. Photo by J.A. Naranjo. (B) Aerial view of the 1994 eruption of Llaima volcano. Photo by H. Moreno.

during the last glaciation. This old edifice suffered a huge collapse at *c.* 13.7 ka during a large explosive eruption (*c.* 24 km<sup>3</sup>), that generated the Curacautín Ignimbrite, a series of pyroclastic flows, basaltic andesite in composition, reaching up to more than 70 km from their source (Moreno & Naranjo 1989, 1991, 2003). This explosive stage continued until about 7 ka with a series of andesitic to dacitic pyroclastic flows, surges and Plinian tephra fallout deposits (Fig. 5.16). The second stage of evolution was built on top of the western and northern slopes of the old volcano, with many parasitic centres. Lavas and pyroclasts have basaltic andesite to andesitic composition. The present composite stratovolcano began to form after 3 ka and is largely composed of lavas and pyroclastic deposits of basaltic and basaltic andesitic composition. There are almost 40 parasitic centres located on its western and northeastern flanks, including pyroclastic cones and minor fissural centres, mostly aligned along a 25-km-long SW–NE arc structure.

The main hazard related to Llaima volcano corresponds to the generation of lahars due to ice/snow melting of its ice-cap during an eruption from either the central or a flank vent (Moreno & Naranjo 2003). Emission of lava flows (up to 30 km long) and tephra fallout (mainly distributed towards the east) are also two important hazards that could damage villages located on the lower flanks of the volcano. Large explosive eruptions have not occurred at Llaima since the generation of the Curacautín Ignimbrite at *c.* 13.7 ka, and another complex Plinian eruption at *c.* 9 ka (Naranjo & Moreno 1991, 2005).



**Fig. 5.16.** Late Pleistocene to Holocene pyroclastic deposits derived from Llaima volcano, including the large-volume mafic Curacautín ignimbrite at the base. Photo by J. A. Naranjo.

Nevertheless, the remote possibility of the generation of pyroclastic flows has to be considered during severe Strombolian to Subplinian eruptions (Moreno & Naranjo 1989, 1991, 2003).

**Villarrica (39.5°S, 71.9°W, 2847 m).** This is a large ( $c. 250 \text{ km}^3$ ) Middle Pleistocene–Holocene compound volcano (Fig. 5.17), located on the western edge of the Villarrica–Quetupillán–Lanín volcanic chain, which is oblique to the main volcanic chain of the SVZ (Fig. 5.8). Villarrica has had more than 30 reported eruptions in historic times (Petit-Breuilh 1994; Petit-Breuilh & Lobato 1994; Simkin & Siebert 1994). The most important eruptive events in recent times occurred in 1948–49, 1963–64, 1971–72 and 1984.

The evolution of Villarrica volcano has been divided into three stages according to geochronological, stratigraphical and morphostructural criteria (Clavero & Moreno 2004; Moreno & Clavero 2006). In its early evolution (Villarrica 1 unit, middle to upper Pleistocene) an ancestral stratocone was built, mainly with basaltic to basaltic andesite lavas and fallout deposits. At  $c. 100 \text{ ka}$  this ancestral edifice partially collapsed, generating an elliptical caldera structure, 6.5 km by 4.2 km in diameter. Subglacial basaltic andesite lavas and dacitic domes and dykes were generated during the Llanquihue Glaciation (95–14 ka), as well as a series of pyroclastic flows and both basic and acid tephra fallout deposits, which are mainly preserved on the lower western flank of the volcano (Clavero & Moreno 2004; Gaytán *et al.* 2005), although it is not clear if an edifice was formed during this period. A second caldera collapse, nested in the previous structure, occurred at  $c. 13.7 \text{ ka}$  (caldera 2), with the generation of a series of pyroclastic flows, including the large-volume Licán Ignimbrite ( $c. 10 \text{ km}^3$ ; Clavero 1996; Clavero & Moreno 1994, 2004), marking the beginning of an

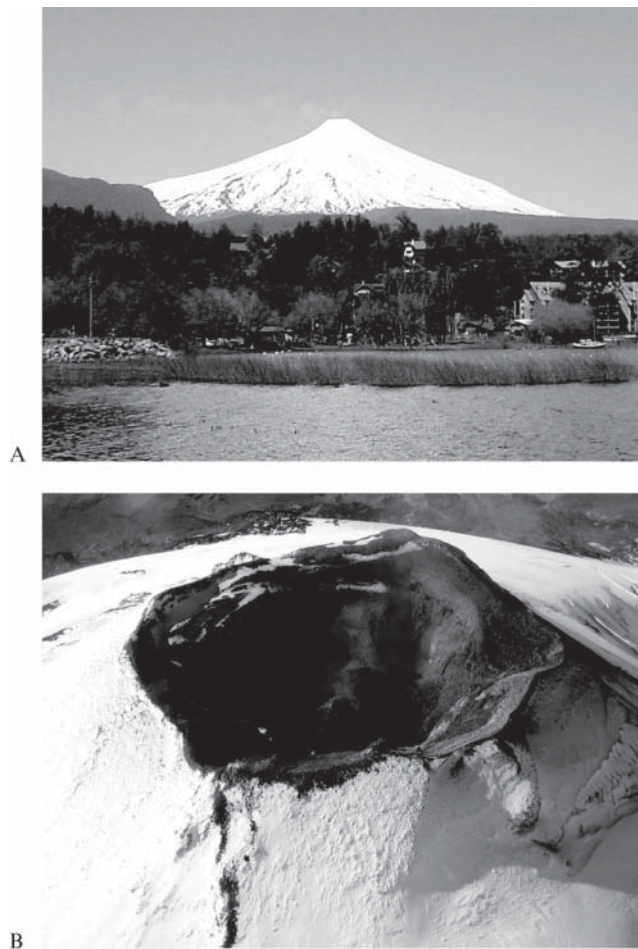


**Fig. 5.17.** (A) Villarrica volcano looking SW from Pucón. Note the gas plume dispersed towards the east. (B) The partially covered lava lake, in April 2005, below a small cone inside the Villarrica crater. The crater lava lake is a feature that apparently has persisted since the 1971–72 eruption (Calder *et al.* 2004; Witter *et al.* 2004). Photos by J Clavero.

explosive phase, which seems to have continued to the present day. A new stratocone located on the northwestern rim of calderas 1 and 2 was formed through successive effusive and explosive eruptions (Villarrica 2 unit, 14–3.7 ka). At  $c. 3.7 \text{ ka}$  this stratocone partially collapsed, forming a smaller summit caldera (caldera 3) associated with the Pucón Ignimbrite eruption (Clavero 1996; Clavero & Moreno 2004; Silva *et al.* 2004), which marked the end of Villarrica 2 unit. Soon after the collapse a new stratocone started to build within the summit caldera. This new cone has been built through successive effusive and explosive eruptions (Villarrica 3 unit, 3.7 ka to present). The last large explosive event at Villarrica volcano occurred  $c. 530$  years ago (Moreno & Clavero 2006), with the formation of a pyroclastic flow directed towards the northeastern flank of the volcano. In total, the post-glacial eruptive history of Villarrica volcano (13.7 ka to present) has produced at least 15 small to large-volume pyroclastic flows and surges.

Historic eruptions that have occurred at Villarrica volcano have been mainly Hawaiian to Strombolian (Petit-Breuilh 1994; Petit-Breuilh & Lobato 1994; Moreno 1993; González-Ferrán 1995; Clavero & Moreno 2004). The main related hazards are generation of lahars, lava flows, tephra fallout and small-volume pyroclastic flows. Lahars, which are the only hazard that have produced casualties in Villarrica's history, can be generated by ice/snow melting by lava or pyroclastic flows on top of the permanent ice-cap (Rivera *et al.* 2006), and could



be directed all around the volcano (Moreno 2000), reaching extensively populated areas, such as the towns Pucón and Villarrica on its northern foot. Tephra fallout, produced during Strombolian eruptions, could affect areas located mainly towards the east, according to the prevailing low to medium-altitude winds in the area, although it could be directed towards different zones when unusual winds blow. Lava flows, as lahars, can be directed almost all around the volcano and reach distances of up to 25 km. Finally, but not least important, Villarrica volcano has generated abundant pyroclastic flows ranging from small to large ignimbrites. The last of these highly explosive eruptions occurred only around 530 years ago (Moreno & Clavero 2006), indicating that such an explosive eruption could be generated at any time in the future, threatening the highly populated areas near the volcano, which increase their population up to three-fold in the summer. Small-volume pyroclastic flows, less than 5 km long, were generated during the 1948–49 eruption. Larger explosive eruptions may produce flows that reach more distal areas.

A lava lake in Villarrica's crater (Fig. 5.17B; Calder *et al.* 2004; Witter & Delmelle 2004; Witter *et al.* 2004) also generates a hazard to the numerous tourists who climb to the crater almost every day. The occurrence of small explosions, and emissions of SO<sub>2</sub> and HCl that exceed recommended limits, threaten the safety and health of the visitors (Witter & Delmelle 2004).

**Quetupillán (39.5°S, 71.7°W, 2360 m).** This is a Pleistocene to Holocene compound stratovolcano formed by two nested calderas, and a series of domes and pyroclastic cones (Pavez 1997; Naranjo 2004; Pavez *et al.* 2004). An extensive post-glacial (<15 ka in the area) pyroclastic sequence, which includes pyroclastic flow, surge and tephra fallout deposits, has been recognized (Naranjo 2004; Lara & Moreno 2004). Dacitic domes and coulées surround the caldera structures, while the pyroclastic cones are aligned NE–SW (Pavez 1997). At least one historic eruption has been reported, which occurred in 1872 (Simkin & Siebert 1994). Although no large populated areas surround the volcano, a large explosive eruption, such as those that occurred after the last glaciation, could generate pyroclastic flows that would reach inhabited areas.

**Mocho–Choshuenco volcanic complex (39.9°S, 72°W, 2430 m).** This is a Pleistocene–Holocene complex, formed by the remnants of an old edifice (Choshuenco peak; Fig. 5.18) and a small stratocone (Mocho) built within a caldera structure. The evolution of the complex probably started in the late Pleistocene with the emission of a series of basaltic andesite to andesite lavas. In the early post-glacial period (*c.* 11 ka) an



Fig. 5.18. Choshuenco volcano viewed from the NW. Photo by J. Clavero.

explosive phase started with the generation of large-volume Plinian fallouts: the Pirehueico (Naranjo *et al.* 2001a, b) and Neltume (Echegaray *et al.* 1994; Echegaray 2004; Naranjo *et al.* 2001a, b) Plinian tephra-fall deposits, of dacitic to andesitic composition. The Neltume eruption tephra-fall deposits covered an area of more than 4000 km<sup>2</sup>, reaching distances over 50 km to the north. One of these eruptions probably produced the partial collapse of the ancestral edifice forming a caldera. The explosive activity continued in the Holocene with the generation of a series of pumice- and scoria-rich pyroclastic-flow, dry and wet surges, and tephra fallout deposits both of andesitic and dacitic composition (Echegaray 2004; Pérez 2005). Simultaneously, a series of flank cones (Fuy series) were formed on the lower northeastern flank, and a small stratocone with lavas and tephra fallout layers started to infill the caldera depression. The last explosive eruption of Mocho–Choshuenco volcano occurred in 1864, with the formation of a highly destructive pyroclastic surge towards the western flank of the volcano. According to its post-glacial and recent eruptive history, Mocho–Choshuenco volcano must be considered one of the most hazardous volcanoes of the SVZ, and one of the most highly explosive (Naranjo *et al.* 2001a, b).

The major hazards related to Mocho–Choshuenco are the generation of highly explosive eruptions with the formation of pyroclastic flows and/or surges as have occurred several times in its very recent history. Tephra fallout could reach populated areas in Argentina (to the east) affecting both tourism and agriculture. Another hazard is related to the permanent ice-cap that fills the caldera depression (Rivera *et al.* 2005), as it is a source for lahar generation. Finally, it is likely that new flank cones will form with their associated lava flows, especially on its northeastern lower flank, as has been recurrent in the last 6000 years.

**Carrán–Los Venados (40.4°S, 72.1°W, 709 m).** This forms a cluster of mainly Holocene basaltic and basaltic andesite pyroclastic cones and maars which form a NE-trending alignment (Moreno 1977; Rodríguez *et al.* 1997; Campos *et al.* 1998; Lara *et al.* 2006b). Eruptions observed during the twentieth century occurred in 1907, 1955 (when fine ash reached the city of Santiago, more than 900 km to the north) and 1979.

**Cordón Caulle–Puyehue (40.5°S, 72.2°W).** This middle Pleistocene–Holocene volcanic complex comprises the Cordillera Nevada caldera, Cordón Caulle fissure system and the Puyehue volcano (2240 m) in a NW-trending alignment (Moreno 1977; Lara *et al.* 2006a, b) that has emitted voluminous Holocene andesitic to dacitic pyroclastic ejecta. A remarkable fissure eruption of rhyodacites followed the high-magnitude (9.5) earthquake in 1960 (Lara *et al.* 2004b). This complex has an active geothermal field, which has been recently studied as a geothermal prospect (Sepúlveda *et al.* 2004).

**Osorno (41.1°S, 72.5°W, 2652 m).** This is a Pleistocene and Holocene stratovolcano (Moreno *et al.* 1979, 1985) with a field of Holocene basaltic pyroclastic cones on its flanks (Fig. 5.19). At least ten historical eruptions have been reported, the last in 1835 when a NE-trending system of fissures and cones formed (López-Escobar & Parada 1991; Petit-Breuilh 1999).

Osorno has the potential to produce lava flows that could possibly affect almost any of the areas all around the volcano. Lava flows might be erupted from either the central cone or the parasitic scoria cones on the volcano's flanks and could flow up to 12 km from the vent. However, lahars are the most important volcanic hazard associated with Osorno volcano, based on their recurrence both in the historic and geological record. Scenarios for the generation of lahars vary according to the time of the year because of changes in the seasonal snow-covering thickness. Thus, in summer the Petrohué valley could be affected by lahars reaching about 80 × 10<sup>6</sup> m<sup>3</sup> in size, but in winter the volume could increase to about 200 × 10<sup>6</sup> m<sup>3</sup>.





Fig. 5.19. Osorno volcano viewed from the south. Photo by L.E. Lara.

Although pyroclastic flows are not the most common volcanic product in Osorno's recent eruptive history, their widespread distribution together with their highly destructive character make them an important hazard for the areas surrounding the volcano. Thus although the possibility of generation of a pyroclastic flow is very low, it nevertheless represents the most dangerous type of threat posed by Osorno volcano. According to the prevailing high-altitude wind directions (from NW to SE) tephra-fall hazards could affect areas located mainly to the ESE of the volcano. Although there are no important human settlements towards the east in Chile, a highly explosive eruption could produce tephra fallout deposits that could reach more populated areas such as San Carlos de Bariloche in Argentina.

**Calbuco (41.3°S, 72.6°W, 2015 m).** This is a Pleistocene–Holocene compound andesitic volcano (López-Escobar *et al.* 1992, 1995b; Hickey-Vargas *et al.* 1995). A sector collapse occurred during the early post-glacial period, generating a large avalanche which flowed to the north (Moreno *et al.* 1985), and an andesitic dome grew inside the collapse amphitheatre. Eleven historic eruptions have been recorded, the last in 1961 (Petit-Breuilh 1999).

Calbuco has produced blocky lava flows in both pre-historic and historic eruptions. Similar eruptions could affect areas located mainly toward the NE and SE of the volcano. The lava flows could be erupted from the central dome, but because of their high viscosity would not be expected to reach >9 km from the vent. Lava flows could potentially block the Caliente river valley forming a dam and an unstable and hazardous lake that could produce violent flooding downstream.

As Calbuco volcano is highly explosive, ballistic pyroclasts can reach long distances around the volcano, and pumice bombs up to 10 cm in diameter have been found in deposits 24 km east of the volcano. During the 1893–95 eruptive cycle, bombs up to 30 cm in diameter were thrown out to 8 km from the vent, killing cattle and causing forest fires. Dispersal of ash plumes would cause tephra fall affecting areas located mostly on the east and southeastern side of the volcano. Tephra fallout deposits could also reach more populated areas further to the east such as El Bolsón, San Carlos de Bariloche and Villa La Angostura in Argentina.

Historic eruptions of Calbuco, like that during 1893–95, have been explosive, but have produced only small-volume pyroclastic flows/surges and block-and-ash flows. However, the geological record indicates that the average recurrence of

larger pyroclastic flows is less than 500 years, and the current evolution of the volcano suggests that the main central dome is still growing. For this reason, the possible future generation of a large pyroclastic flow ( $\geq 1 \text{ km}^3$ ) that could cover an area greater than  $1000 \text{ km}^2$  represents the most dangerous type of threat from Calbuco volcano.

Lahars have also been one of the most dangerous and destructive processes associated with eruptions of Calbuco. Lahars from Calbuco are generated in two different ways: by sudden melting of ice and seasonal snow or by mixing of block-and-ash flows with stream waters. The eruptive historic record for Calbuco includes the formation of 'hot lahars' toward the NE, SE and south of the volcano, that rapidly indurate, suggesting that they are generated by mixing of pyroclastic flows/surges and block-and-ash flows with river waters (Moreno & Naranjo 2004). Lahars generated by melting of ice and snow have also travelled down through the main valleys on the volcano slopes, and spread over wider areas when reaching lowlands, especially close to the shores of Llanquihue and Chapo lakes. As with Osorno, the scenario for an eventual lahar generation during an eruption varies significantly according to the time of the year because of variations in the seasonal snow-covering thickness. For example, in summer the Blanco and Hueñuhueñu river valleys could be affected by lahars reaching a volume of about  $3 \times 10^6 \text{ m}^3$ , although in winter the volume could increase drastically to about  $82 \times 10^6 \text{ m}^3$ .

#### The SSVZ

The SSVZ consists of 13 Quaternary volcanoes forming a narrow chain that crops out completely in Chile (Fig. 5.8; Stern *et al.* 1976b; Futa & Stern 1988; López-Escobar *et al.* 1993; D'Orazio *et al.* 2003; Naranjo & Stern 2004). Numerous minor eruptive centres also occur in the SSVZ along the LOFS and subparallel faults (Demant *et al.* 1994). The larger composite stratovolcanoes of the SSVZ include Yate, Hornopirén, Michinmahuida, Corcovado, Yanteles, Melimoyu, Mentolat, Cay and Macá (Fig. 5.20). Hudson volcano is a 10-km-diameter caldera. Huequi is a relatively small cinder cone, but may be part of larger eroded complexes, and Hualaihué–Cordón Cabrera is also a small pyroclastic cone aligned along a fissure system which includes eroded volcanic necks, domes and cones. Chaitén is formed by a rhyolite dome inside an explosion crater or small caldera (Fig. 5.21) located immediately to the west of the western flanks of the Michinmahuida complex, the largest volcano in the SSVZ.

Michinmahuida had historic eruptions in 1742 and 1834–35, and Hudson had an event that produced a large lahar in 1971



Fig. 5.20. Maca volcano viewed from the west across the Moraleda channel. Photo by C.R. Stern.

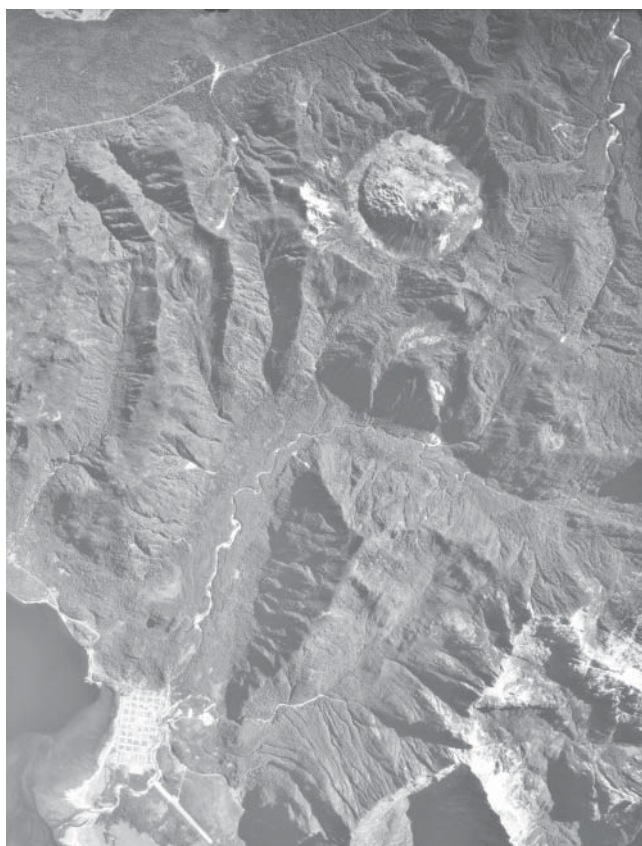


**Fig. 5.21.** Vertical aerial photo of the Chaitén rhyolite dome inside a small explosion crater or caldera located a few kilometres NW of the town of Chaitén.

(Best 1992), followed by a large explosive eruption in 1991 ( $> 3.6 \text{ km}^3$ ; Naranjo *et al.* 1993b). All the other SSVZ volcanoes have had Holocene eruptions, except perhaps Cay volcano (Naranjo & Stern 2004). At least ten of the SSVZ centres have had medium to large explosive eruptions during the Holocene, namely Yate, Huequi, Chaitén, Michinmahuida, Corcovado, Yanteles, Melimoyu, Maca, Mentolat and Hudson (Naranjo & Stern 1998, 2004). The towns of Chaitén, Futaleufú, Puerto Aisén, Coihaique, Puerto Ibáñez and Chile Chico in Chile, as well as Esquel in Argentina, occur within the  $> 10 \text{ cm}$  tephrafall isopach of at least one of these eruptions. Puerto Ibáñez was significantly impacted by both ashfall and volcanic ash washed into General Carrera lake by the Ibáñez river after the 1991 eruption of Hudson volcano (Fig. 5.22; Naranjo *et al.* 1993b), and the port remains shut down as a result of this eruption. Hudson also had two very large pre-historic Holocene explosive eruptions, including one at *c.* 6700 years BP that may be among the largest Holocene explosive eruptions in the SVZ ( $> 18 \text{ km}^3$ ; Naranjo & Stern 1998). This eruption deposited  $> 15\text{-cm}$ -thick tephra layers as far south as Tierra del Fuego (Fig. 5.23; Stern 1991d, 2007). Hudson is anomalous in the SSVZ with regard to the number of large-volume explosive Holocene eruptions it has produced, which may relate to its proximity to the Chile triple-junction.

Because of the high precipitation and cool climatic conditions in southern Chile, the volcanic centres of the SSVZ in general have a great deal of snow cover, which increases lahar potential, as illustrated by lahars generated by a thermal event that caused the melting of the glacial fill inside the caldera of Hudson volcano in 1971 and 1991 (Best 1992; Naranjo *et al.* 1993b). Although the SSVZ volcanoes are generally remote



**Fig. 5.22.** Boat docked at Puerto Ibáñez port, now permanently landlocked in volcanic ash that was washed into General Carrera Lake by the Ibáñez River after the August 1991 eruption of the Hudson volcano. The delta formed by this ash prograded the post-eruption coast more than 100 m into the lake. Photo by M. Villouta.



**Fig. 5.23.** A 20-cm-thick tephra layer in Tierra del Fuego derived from the 6700  $^{14}\text{C}$  years BP explosive eruption of the Hudson volcano located  $> 1000 \text{ km}$  to the north (Stern 1991d, 2007). This eruption was one of the largest ( $> 18 \text{ km}^3$ ; Naranjo & Stern 1998) Holocene explosive eruptions of any volcano in the SVZ. Photo by C.R. Stern.

from local population centres, the town of Chaitén is located directly at the base of Chaitén volcano (Fig. 5.21), which has had at least one Holocene explosive eruption, and drainage systems from Michinmahuida volcano also pass through Chaitén.

### AVZ volcanoes of southernmost Chile (C.R.S.)

The AVZ volcanic segment in southernmost Chile occurs between latitudes  $49^\circ\text{S}$  and  $55^\circ\text{S}$  (Fig. 5.24). It includes only six volcanic centres: Lautaro ( $49^\circ\text{S}$ ), Viedma ( $49.4^\circ\text{S}$ ), Aguilera ( $50.2^\circ\text{S}$ ), Reclus ( $51^\circ\text{S}$ ), Monte Burney ( $52.3^\circ\text{S}$ ) and Cook Island ( $54.9^\circ\text{S}$ ). The AVZ was first recognized as a separate Andean volcanic segment in 1976 (Stern *et al.* 1976b), while the Cook Island volcanic complex, the southernmost in the Andean Quaternary arc, was not discovered until 1978 (Puig *et al.* 1984; Martinic 1988) and Reclus volcano was accurately located only in 1987 (Harambour 1988). Lautaro, Viedma and Aguilera volcanoes occur within the region of the southern Patagonian



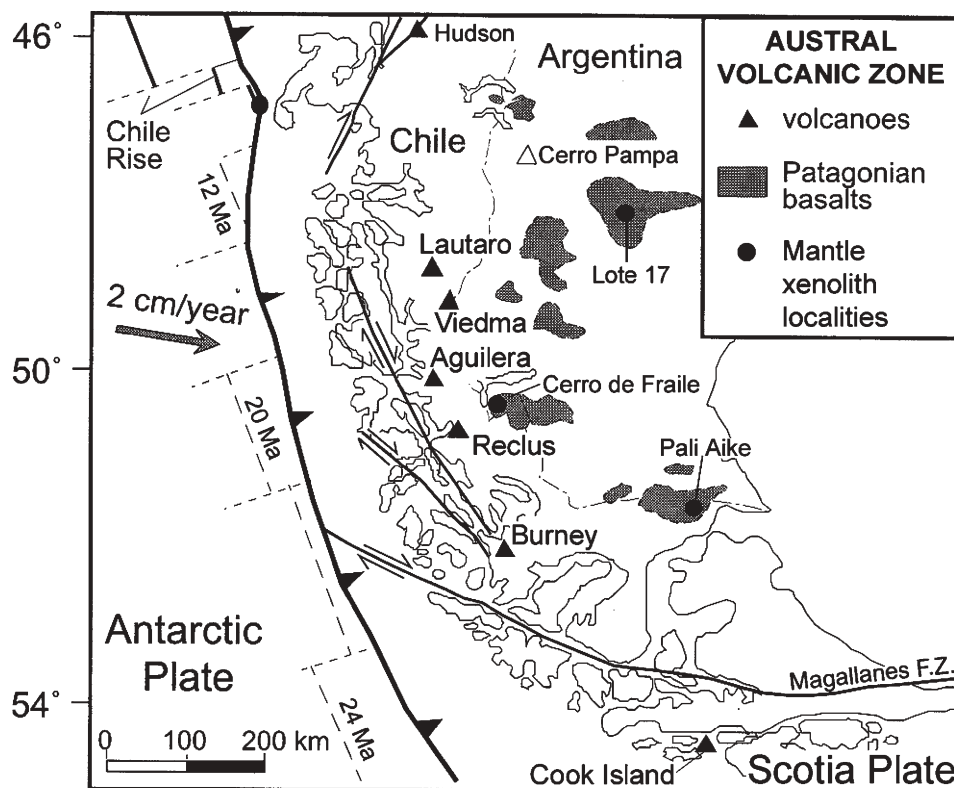


**Fig. 5.24.** Map of the location of the six volcanic centres that form the Austral Volcanic Zone, outcrops of the Patagonian plateau basalts to the east, and plate boundaries in the region.

ice-cap, where the border between Chile and Argentina is as yet unresolved, but the other three centres occur in Chile.

#### *Geological and tectonic setting*

The AVZ results from the subduction of the Antarctic Plate below the South American Plate. It is separated from the SVZ by the Patagonian gap in active volcanism just south of the Chile Ridge–Trench triple-junction (46–49°S; Figs 5.1 & 5.24), where very young oceanic lithosphere (<6 Ma) is being subducted. The age of the Antarctic Plate at the trench changes from 12 Ma below the northern part of the AVZ to 24 Ma in the south. Convergence velocities between the Antarctic and South American plates are relatively low (2–3 cm/year), and there is no Benioff zone of seismic activity associated with subduction of this oceanic plate, possibly because the slow rate of convergence and young age of the oceanic plate may cause the subducted slab to be several hundreds of degrees hotter than in more typical subduction environments (Peacock *et al.* 1994). Because of the lack of seismicity, the geometry of the subducted slab and mantle wedge below the AVZ cannot be determined. The convergence direction changes from nearly orthogonal in the north to oblique in the south. Strike-slip plate motion takes place at the latitude of Cook Island, which occurs on the Scotia microplate (Forsyth 1975), south of the Magallanes fault system (Fig. 5.24).

The southernmost Andes consist of Late Palaeozoic to Early Mesozoic metamorphic basement. Mesozoic and Cenozoic mafic, intermediate and silicic igneous rocks, as well as sedimentary rocks, were deformed and uplifted beginning in mid- to Late Cretaceous times (Bruhn & Dalziel 1977). Cook Island volcano directly overlies plutons of the Patagonian batholith, and Mt Burney, Reclus and Aguilera volcanoes occur along the eastern margin of the batholith. Viedma and Lautaro volcanoes occur within the area of the Patagonian ice-cap, which impedes knowledge of their bedrock geology. Base

elevations of AVZ volcanoes are less than a few hundred metres above sea level, and summit elevations are less than 3600 m. This suggests that crustal thickness is <35 km. Lower crustal xenoliths found in the Patagonian plateau basalts are pyroxene + plagioclase granulites, without garnet, consistent with a relatively thin crust below southernmost South America (Selverstone & Stern 1983).

The Chile Ridge was subducted below the southernmost Andes during late Miocene times, resulting in the development of a slab window and extensive basaltic plateau volcanism in southern Patagonia prior to the reinitiation of subduction and AVZ arc magmatism (Ramos & Kay 1992; D’Orazio *et al.* 2000, 2001; Gorrington & Kay 2001). Ridge subduction may have also caused subduction erosion along the continental margin (Bourgeois *et al.* 1996, 2000; Polonia *et al.* 1999; Guivel *et al.* 2003, 2006), and the western edge of the Patagonian batholith lies much closer to the trench south of the Chile Ridge–Trench triple-junction than north of it (Cande & Leslie 1986). These authors also suggest that active subduction erosion is occurring in conjunction with the subduction of the Chile Ridge at 46°S, and presumably west of the AVZ as the locus of subduction of this spreading ridge migrated northwards during the Miocene.

#### *AVZ volcanoes and volcanic hazards*

The Cook Island volcanic complex consists of a group of post-glacial domes (Fig. 5.25; Puig *et al.* 1984; Heusser *et al.* 1989–90), some of which also occur on nearby Londonderry and Kelvin Islands (Dreher *et al.* 2005). All the other AVZ volcanoes are glaciated stratovolcanoes. Monte Burney (Fig. 5.26) has a small summit crater and a steep vertical northern wall, which may have formed from glacial erosion, a lateral blast or sector collapse. A broad plain to the NE, east and SE of Mt Burney is formed by a >5-m-thick section of Holocene pyroclastic flows. Small isolated outcrops of volcanic rocks



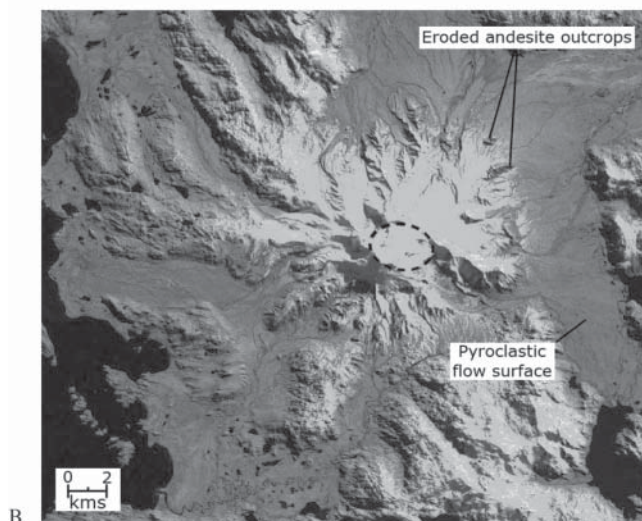


**Fig. 5.25.** One of eight to ten small domes that make up the Cook Island volcanic complex, the southernmost in the Andean chain. Photo by S. Dreher.

engulfed by these flows (Fig. 5.26B) may represent highly eroded pre-Holocene Mt Burney lavas. However, these outcrops have not been dated. Other evidence for pre-Holocene volcanic activity in the AVZ is provided by 0.17 Ma K–Ar dates from Lautaro volcano (Orihashi *et al.* 2004).



A



B

**Fig. 5.26.** (A) Monte Burney volcano viewed from the NW. Photo by C.R. Stern. (B) Satellite image of Monte Burney showing its small summit crater (dashes) and the large areas on the NE, east and SE flanks of the volcano covered by Holocene pyroclastic flows > 5 m thick.

Lautaro is also the only centre in the AVZ with a documented historic eruption, which occurred in 1959 (Martinic 1988). However, tephra records indicate that each of the five AVZ stratovolcanoes has had Holocene explosive activity (Stern 1990b, 1992, 2000, 2007; Kilian *et al.* 2003; Motoki *et al.* 2003, 2006). Mt Burney, Recluse and Aguilera have each had large (> 2.5 km<sup>3</sup>) late glacial and/or Holocene explosive eruptions, as well as a number of smaller eruptions. Although all the AVZ volcanoes are remote from any population centre in southernmost Patagonia, such as Punta Arenas, Puerto Natales and Calafate, recurrence of an eruption as large as one of the larger Holocene events could produce significant tephra-fall in the area of these cities, as well as affecting the livestock ranching industry, as did the 1991 eruption of Hudson further north in Patagonia. Nevertheless, the presence of only six volcanic centres in a region extending over six degrees of latitude, and the relatively few documented explosive eruptions, suggests that magma production rates and the potential for explosive eruptions in the AVZ are less than in the SVZ, presumably as a result of the lower plate convergence and subduction rates below the AVZ (Stern 1990b, 2000, 2007).

### Petrogenesis of the Quaternary Andean volcanoes of Chile (C.R.S., L.L.-E., H.M. & M.A.P.)

Andean magmatism is initiated by the dehydration and/or melting of the subducted oceanic lithosphere resulting in the addition of subducted components into, and melting of, the overlying mantle wedge (Thorpe 1984; Stern 2004). In this sense the initial subcrustal stages of generation of Andean magmas are similar to magma-generation processes in oceanic convergent plate-boundary island arcs. In fact, tholeiitic and high-Al basalts from the volcanic front of the Central SVZ of the Andes, where the crust is < 35 km thick, have isotope and trace-element ratios similar to oceanic island arc basalts, and they have not obviously assimilated continental crust (Hickey-Vargas *et al.* 1984, 1989; Hickey *et al.* 1986; Futa & Stern 1988).

However, differences in isotopic composition of volcanic rocks from the Northern SVZ and CVZ of the Andes, compared with those erupted in the Central SVZ and oceanic island arcs, do indicate the participation of continental crust and/or subcontinental mantle lithosphere in the formation and evolution of the NSVZ and CVZ Andean magmas. This may occur during interaction of magmas derived in the subarc asthenospheric mantle wedge with continental lithosphere (Rogers & Hawkesworth 1989; Stern & Kilian 1996; Hickey-Vargas *et al.* 2002), by intracrustal assimilation (AFC or MASH processes; James 1984; Hildreth & Moorbath 1988; Davidson *et al.* 1991), and/or by source region contamination of subarc mantle by subducted continental components (Stern *et al.* 1984b; Stern 1988, 1990a, 1991b; Stern & Skewes 1995; Kay *et al.* 1999, 2005). Relative roles of each process differ in the different Andean volcanic zones as a function of variations in the thickness and composition of the continental crust and rates of subduction erosion of the continental margin.

### SVZ petrography, geochemistry and petrogenesis

Along-arc petrochemical variations in the SVZ are discussed for each zone, beginning with the CSVZ and SSVZ, since volcanic rocks and magma-generation processes in these two zones are most similar to oceanic island arcs.

#### The CSVZ and SSVZ

In the Central and Southern SVZ, where the crust is relatively thin (< 35 km), tholeiitic and high-Al basalts and basaltic andesites are the dominant rock types erupted from both stratovolcanoes and many minor eruptive centres (López-Escobar

*et al.* 1977, 1993, 1995a; Hickey-Vargas *et al.* 1984, 1989; Hickey *et al.* 1986; Gerlach *et al.* 1988; Futa & Stern 1988), although andesites, dacites and rhyolites do occur. Two main types of basaltic rocks, one relatively K-depleted ( $K_2O < 1\%$ ) and the other relatively K-enriched ( $K_2O = 1$  to  $> 1.5\%$ ), have been distinguished in both the stratovolcano and MEC of the CSVZ and SSVZ (López-Escobar *et al.* 1995a). Even the most primitive basalts show evidence of having undergone fractional crystallization, as their MgO contents are  $< 11\%$ , and their Ni and Cr abundances both lower than those expected in mantle-derived primary magmas. A remarkable feature of the rocks in these two SVZ segments is that olivine phenocrysts are present in the entire suite, including iron-rich olivine in some of the few rhyolites. Plagioclase phenocrysts are also ubiquitous, although their modal percentage ranges from only about 1–10% in MEC volcanic rocks to 20–50% in composite stratovolcano products. Orthopyroxenes appear in intermediate to silicic rocks ( $> 57\%$   $SiO_2$ ). An important feature of the CSVZ volcanic segment is that most silicic rocks lack hydrous minerals such as amphibole and mica. Indeed, a key difference that distinguishes the SSVZ from the CSVZ is the presence, in the most silicic SSVZ rocks, of hydrous minerals like hornblende (in rocks with  $> 59\%$   $SiO_2$ ) and scarce biotite, the latter only in the Chaitén rhyolites.

Tectonism seems to control whether basaltic magmas reach the surface or evolve to more differentiated products at crustal levels. Most late Pleistocene and Holocene volcanic centres defining NE-trending alignments, including both composite stratovolcanoes  $\pm$  MEC, contain mainly basaltic to basaltic andesite lithologies, such as seen in the Osorno–Puntiagudo–Cordón Cenizos volcanic chain. This is consistent with a short residence time of magmas in the crust (Tormey *et al.* 1991b), resulting in limited contamination and fractionation of mantle-derived magmas. On the other hand, volcanic edifices controlled by NW-trending fractures and faults, such as in the Villarrica–Quetupillán–Lanín and Puyehue–Cordón Caulle volcanic chains, have more differentiated compositions, including rhyolites.

Sr, Nd, Pb and O isotopic data for CSVZ and SSVZ basalts preclude any significant assimilation of continental crust. Detailed studies of these basalts therefore provide information on the genesis and chemical composition of mafic mantle-derived Andean magmas that have not interacted extensively with continental crust, and thus a 'baseline' for evaluating the extent of crustal interaction in other segments of the Andean arc. These studies have concluded that CSVZ and SSVZ basalts form by melting of the subarc mantle contaminated by fluids derived from the dehydration of the subducted oceanic lithosphere, including sediments. This conclusion is based on: (1) Be isotope data which imply a subducted sediment component in CSVZ basalts (Morris *et al.* 1990; Sigmarsson *et al.* 1990; Hickey-Vargas *et al.* 2002); (2) excess  $^{226}Ra$  over  $^{230}Th$  and  $^{238}U$  over  $^{230}Th$  which both imply addition of slab-derived fluids to the mantle magma source (Sigmarsson *et al.* 2002); (3) Pb isotopic data that suggest Pb is derived from a mixture of mantle and subducted Nazca Plate sediment (Barreiro 1984; Macfarlane 1999); (4) high ratios, compared to oceanic island basalts (OIB), of large-ion lithophile elements (LILE) to rare earth elements (REE; for example Ba/La; Fig. 5.27A), REE to high-field-strength elements (HFSE; for example La/Nb; Fig. 5.27B), and very high ratios of LILE to HFSE (for example Ba/Nb; Fig. 5.27C), which reflect the fact that LILE are more soluble than REE, and REE more soluble than HFSE, and therefore relatively enriched in slab-derived fluids (Hickey-Vargas *et al.* 1984, 1989; Hickey *et al.* 1986); and (5) Sr (Fig. 5.27C), Nd and  $\delta^{18}O$  isotopic values indicating only a small difference between CSVZ and OIB basalts, which implies that the mass of components derived from the subducted slab must be small relative to the mass of the mantle source of these basalts (Hickey-Vargas *et al.* 1984, 1989; Hickey *et al.* 1986; Stern *et al.* 1990).

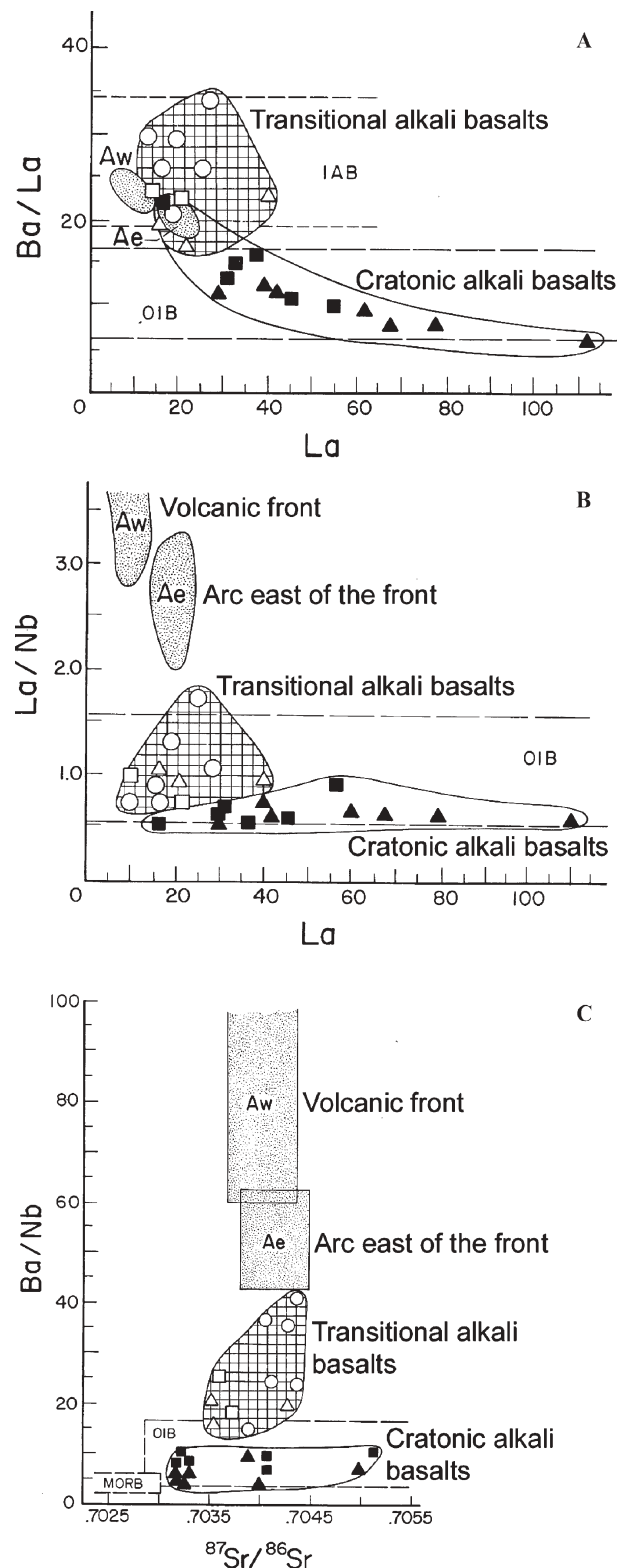


**Fig. 5.27.** (A) Ba/La versus La content; (B) La/Nb versus La content; and (C) Ba/Nb versus  $^{87}Sr/^{86}Sr$ , for samples from along the volcanic front (Aw) of the Central SVZ, CSVZ centres east of the front (Ae), and backarc alkali basalts in areas of Cenozoic arc volcanism (transitional alkali basalts) and cratonic regions that have not experienced Cenozoic arc volcanism (cratonic alkali basalts; Stern *et al.* 1990). Figure illustrates the higher Ba/La, La/Nb and Ba/Nb ratios and La contents from west to east across the CSVZ arc and into the backarc region, interpreted to result from decreasing influx of slab-derived fluids into the subarc asthenospheric mantle wedge, and, as a consequence, decreasing degree of partial mantle melting across the arc.



Decreasing Ba/La, La/Nb and Ba/Nb ratios (Fig. 5.27) in magmas erupted progressively east of the volcanic front in the CSVZ, suggest decreasing input of slab-derived fluids into the mantle source of volcanoes behind the volcanic front as a result of progressive dehydration of the descending slab (Futa & Stern 1988; Stern *et al.* 1990). Decreasing Ba/La and La/Nb across the CSVZ arc are associated with increasing light REE (La; Fig. 5.27A) content and light REE to heavy REE ratios, both of which are interpreted as a measure of the degree of partial melting of the mantle. Thus, as the input of slab-derived fluids into the subarc mantle decreases, so does the percentage of mantle partial melting (Hickey *et al.* 1986; Hickey-Vargas *et al.* 1989; Muñoz & Stern 1989; López-Escobar *et al.* 1995a). Further to the east in the backarc region, alkali basalts derived by relatively low degrees of partial mantle melting exhibit even lower Ba/La, La/Nb and Ba/Nb ratios, similar to OIB (Fig. 5.27), and therefore little or no evidence for input of slab-derived components (Skewes & Stern 1979; Stern *et al.* 1990; Kay *et al.* 1993; Gorrington *et al.* 1997). Also, samples of the South American continental mantle lithosphere, which occur as peridotite xenoliths in backarc alkali basalts, present evidence of metasomatism by slab-derived fluids only when their host basalts were erupted in areas of Cenozoic arc volcanism, such as at Cerro del Fraile, Argentina (Figs 5.24 & 5.35; Kilian & Stern 2002). However, xenoliths in alkali basalts erupted further to the east, in regions with no evidence of Cenozoic arc volcanism such as Pali-Aike, Chile, and Lota 17, Argentina (Fig. 5.24), have been metasomatized by fluids without any slab-derived isotopic or trace-element signature (Stern *et al.* 1986, 1989, 1999; Gorrington & Kay 2001).

Andesites, dacites and rhyolites in CSVZ and SSVZ volcanoes generally have the same isotopic composition as basalts and basaltic andesites, indicating that they formed either by crystal-liquid fractionation without assimilation (Gerlach *et al.* 1988), or assimilated young, isotopically similar crust such as Miocene plutonic rocks (McMillian *et al.* 1989).

#### The NSVZ

Rocks from the NSVZ segment range in composition from basaltic andesite to dacites, with a variable mineralogy that commonly includes plagioclase + clinopyroxene + orthopyroxene + magnetite  $\pm$  hornblende (in rocks with  $\text{SiO}_2 > 57\%$ )  $\pm$  biotite (in rocks with  $\text{SiO}_2 > 60\%$ )  $\pm$  olivine (Hildreth & Moorbath 1988; Sruoga *et al.* 2005). Basalts have not been yet reported, and they are either very rare or simply absent. Rhyolites are scarce, but a large rhyolite pyroclastic flow was erupted in Pleistocene times from the Diamante caldera (Stern *et al.* 1984a).

Geochemically, these have relatively high K, Rb, Sr, Ba, La, Th and U contents and higher Rb/Cs, La/Yb, K/La, Rb/La, Ba/La, Hf/Lu and  $^{87}\text{Sr}/^{86}\text{Sr}$  isotope ratios (Fig. 5.28), but lower K/Rb and  $^{143}\text{Nd}/^{144}\text{Nd}$  (Fig. 5.28) isotope ratios, than either basalts or rocks of similar  $\text{SiO}_2$  content in the CSVZ, indicating incorporation of continental crust in the magmas erupted from these volcanoes (Stern *et al.* 1984b; López-Escobar *et al.* 1985; Futa & Stern 1988; Hildreth & Moorbath 1988; Stern 1988, 1989, 1991b). How this crust is incorporated in these rocks is still under debate. Hildreth & Moorbath (1988) outlined a model of mixing, assimilation, storage and homogenization (MASH) within intracrustal magma chambers. Stern *et al.* (1984b) and Stern (1988, 1991b, c) noted that Sr and Nd isotopic ratios were independent of  $\text{SiO}_2$  in the range from basaltic andesites to dacites, and suggested that isotopic differences between the NSVZ and CSVZ were caused by a northward increase in mantle source region contamination by subducted continental components, due to either (1) a smaller volume of mantle wedge associated with the northward decrease in subduction angle and increase in crustal thickness below the NSVZ; and/or (2) increased subduction erosion caused by the

southward migration of the locus of subduction of the Juan Fernández ridge. Stern (1991b) proposed that a small increase, of from 1% to 2% subducted components, would be sufficient to cause the isotopic differences observed in the NSVZ compared to the CSVZ (Fig. 5.29), while intracrustal assimilation of a mass of crust equal to the mass of mantle-derived basalt would be required to generate the same isotopic change. NSVZ volcanic rocks also have higher La/Yb and lower Yb than CSVZ volcanic rocks, suggesting garnet in their source, which could be in either the mantle (López-Escobar *et al.* 1977; Stern *et al.* 1984b; Stern 1991b) or deep crust (Hildreth & Moorbath 1988).

Stern & Skewes (1995, 2005), Nyström *et al.* (2003) and Kay *et al.* (2005) demonstrated that the isotopic difference between the NSVZ and CSVZ developed during late Miocene and Pliocene times, prior to the migration of the volcanic front to its current position in the Main Cordillera above relatively thick ( $> 45$  km) crust. At the latitude of the Maipo volcano ( $34^\circ\text{S}$ ), progressive temporal changes between the early Miocene and Pliocene occurred in the isotopic composition of mantle-derived olivine basalts, implying changes in the isotopic composition of the mantle source region (Stern & Skewes 1995). Similar progressive changes in isotopic composition occurred between the early and late Miocene further north at latitude  $32^\circ\text{S}$ , and between the early Miocene and Pliocene at latitude  $33^\circ\text{S}$ . The diachronous southward migration of these changes closely follows the southward migration of the locus of subduction of the Juan Fernández Ridge. This suggests that an important part of these changes resulted from increased contamination by crustal components of the mantle source region below the arc, caused by either increased subduction erosion or decreasing subduction angle and mantle volume in association with ridge subduction. In contrast, no isotopic changes occurred in conjunction with the 40 km eastward migration of the front in the Pliocene, and therefore these changes are not correlated with crustal thickness (Stern & Skewes 1995).

#### The TSVZ

The volcanic rocks of this segment vary considerably from one centre to the other, and can even be very different in centres belonging to related group of volcanoes, as seen, for example, in the Planchón–Petroa–Azufre group (Tormey *et al.* 1991a, 1995). Azufre is a bimodal stratovolcano with basaltic andesites of tholeiitic affinities and dacite, Planchón has erupted only tholeiitic basalts and basaltic andesites, while Petroa lavas are mostly calcalkaline basaltic andesites with abundant mixed lavas of andesites and dacites composition. The Tatara–San Pedro–Pellado volcanic complex (Dungan *et al.* 2001) ranges in composition from basaltic andesite to rhyolite, but more than half of the volume of erupted material comprises porphyritic dacite flows. The oldest units of Nevado de Longaví (Sellés *et al.* 2004) are formed by basalts to andesites, while the Holocene ones range from basaltic andesites to dacites. Nevados de Chillán late Pleistocene to Holocene lavas are calcalkaline basaltic andesites to rhyolites (Déruelle & López-Escobar 1999). Finally, Laguna del Maule is also bimodal: the most abundant rock types are basaltic andesites and high-K rhyolites (Frey *et al.* 1984). Large volumes of rhyolites were also erupted in the Chilean TSVZ from the Pleistocene to Recent Calabozos caldera (Hildreth *et al.* 1984; Grunder 1987; Grunder & Mahood 1988) and Puelche volcanic field (Hildreth *et al.* 1999). As noted by Hildreth *et al.* (1999), these TSVZ centres are all located over the fold-and-thrust belt developed along the eastern edge of the Main Cordillera (Folguera *et al.* 2002), although this region of the arc is also characterized by the occurrence of intra-arc extensional basins (Muñoz & Stern 1988). Isotopic data indicate that the generation of these rhyolites involved significant contributions from crustal partial melts.



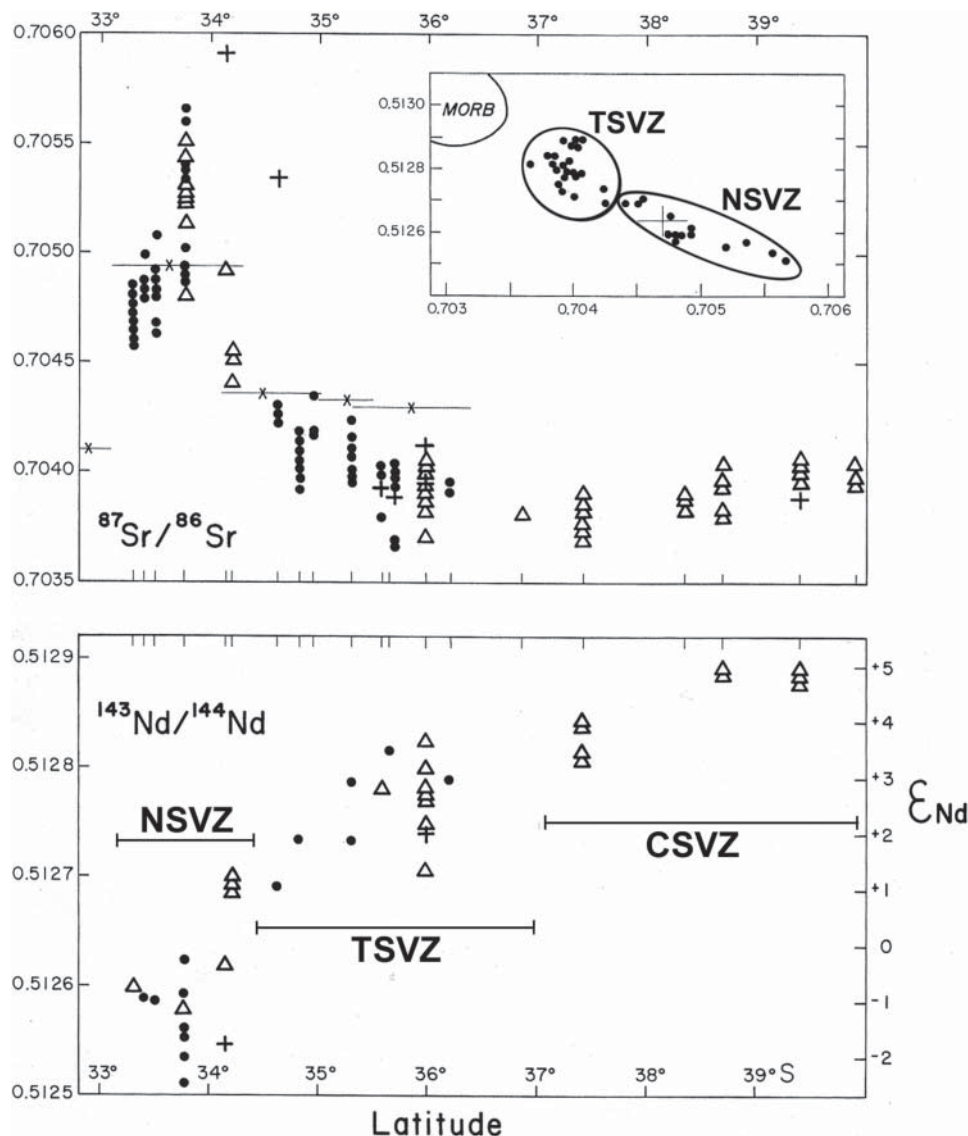


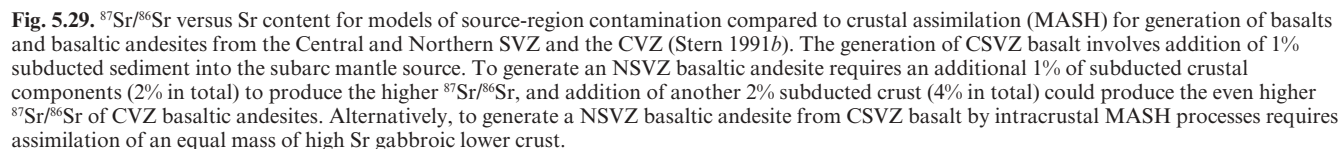
**Fig. 5.28.** Sr and Nd isotopic compositions of SVZ volcanoes in the northern part of the CSVZ, the TSVZ and the NSVZ, modified from Hildreth & Moorbath (1988), illustrating the northward increase in  $^{87}\text{Sr}/^{86}\text{Sr}$  and decrease in  $^{143}\text{Nd}/^{144}\text{Nd}$  ratios.

The Sr and Nd isotopic ratios of the Nevados de Chillán Holocene lavas are among the most primitive within the SVZ arc of the Andes (Dérulle & López-Escobar 1999). Model calculations suggest that the two sources involved in the generation of the most mafic lavas are the asthenospheric mantle, which is the main source, and fluids coming from the subducted slab that enrich the mantle source in some incompatible elements such as K and Rb. The fact that rocks in the basaltic andesite to rhyolite range have similar values of Sr and Nd isotopic ratios, in conjunction with the behaviour of major and trace elements and incompatible element ratios, suggests that the Nevados de Chillán post-caldera magmas evolved through a closed-system fractional crystallization process, and that assimilation of crustal material was limited to <2 %.

At Azufre–Planchón–Petroa (Tormey *et al.* 1991a, 1995), geochemical data suggest that two types of contamination are evident: a lower crustal component which caused increased La/Yb but had no effect on  $^{87}\text{Sr}/^{86}\text{Sr}$ , and an upper crustal component which increased  $^{87}\text{Sr}/^{86}\text{Sr}$  and  $\delta^{18}\text{O}$ . Petroa andesite and dacite lavas formed by magma mixing, indicating that the volcanic system evolved over the past 500 ka from bimodal tholeiitic basalts and dacites (Azufre) to calcalkaline mixed

andesite (Petroa). Banded pumice and preservation of textural disequilibrium suggest that mixing occurred at shallow crustal levels. Thickness of the crust, magma supply rate and crustal temperature are the three main physical controls on compositional variation in this volcanic complex.

In the Tatara–San Pedro–Pellado volcanic complex (Feeley & Dungan 1996; Feeley *et al.* 1998; Dungan *et al.* 2001), three source components are recognized as contributing to parental magmas. These include the subarc asthenospheric mantle (mid-ocean ridge basalt (MORB) source), slab-derived fluids which would be the major source of LILE, and the continental lithosphere including the mantle and/or lower crust. Incompatible element variability in the most mafic rocks is interpreted as a result of source heterogeneity and deep-level processes. Many basaltic andesites to andesite lavas show evidence for magma mixing, and for the underlying magma chamber having been subject to repeated mafic magma replenishment and incorporation of silicic melts. The study of the Tatara–San Pedro complex indicates that open-system processes involving mixing newly arrived magma batches with evolved magmas in conduit–reservoir systems played a more significant role than differentiation in large, long-lived reservoirs.



CVZ magmas have elevated  $^{87}\text{Sr}/^{86}\text{Sr}$  and  $\delta^{18}\text{O}$  (Fig. 5.30; James 1982, 1984), and lower  $^{143}\text{Nd}/^{144}\text{Nd}$  (Fig. 5.31; Wörner *et al.* 1988; Davidson *et al.* 1990, 1991) than SVZ magmas, as

However, not all CVZ volcanoes have correlated variations of Sr, Nd and O isotopes with increasing SiO<sub>2</sub> content. For example, the Nevados de Payachata volcanic group (18°S) exhibits wide variation in elemental composition, but only minor variations in Sr, Nd and Pb isotopic composition. Davidson *et al.* (1990, 1991) explain these chemical and isotopic features through a complex petrogenetic evolution involving primary mantle-derived magmas which are modified by deep crustal interactions to produce magmas with 'baseline' isotopic compositions (Figs 5.30 & 5.31) that are parental to those erupted at the surface. They suggest that these 'baseline'

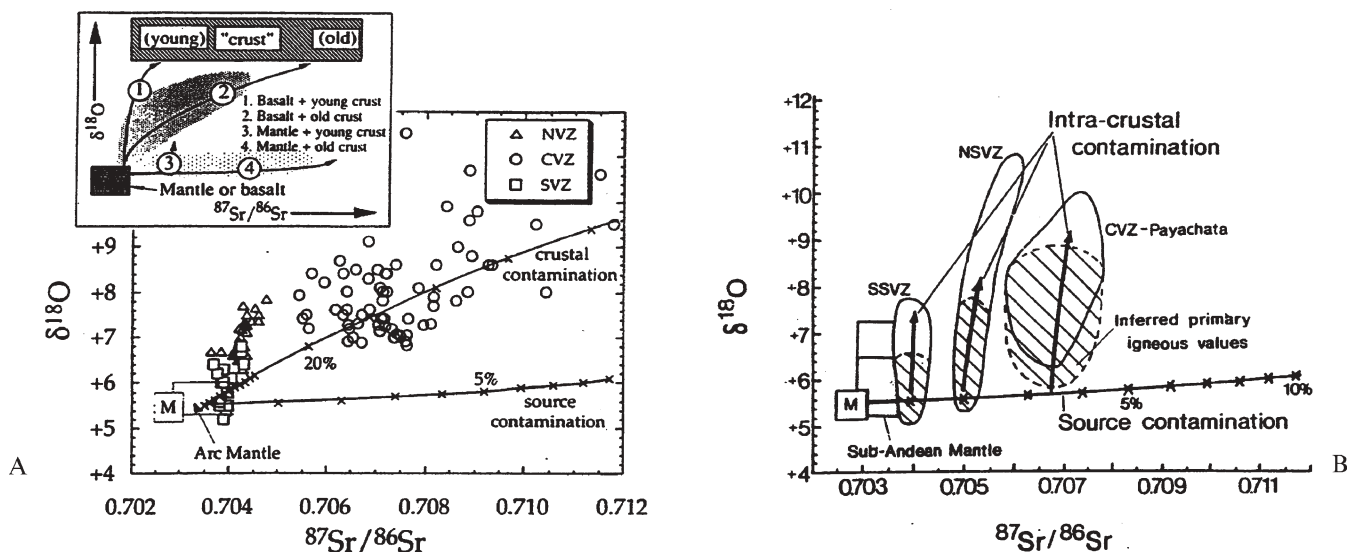


**Fig. 5.30.** Sr versus O isotopes of Andean magmas, modified after (A) Davidson (1991) and (B) Stern (1991c). Each figure illustrates the different trends expected from mantle source contamination, which affects Sr but not O isotopic composition significantly, and intracrustal assimilation, which affects both isotopic systems. As interpreted by Davidson (1991), isotopic values of SVZ versus CVZ volcanic rocks suggested greater intracrustal contamination involving older crust in the CVZ. As interpreted by Stern (1991c), the data suggest changes in the 'baseline' isotopic composition of CVZ relative to SVZ magmas due to greater source-region contamination, followed by intracrustal assimilation in each area.

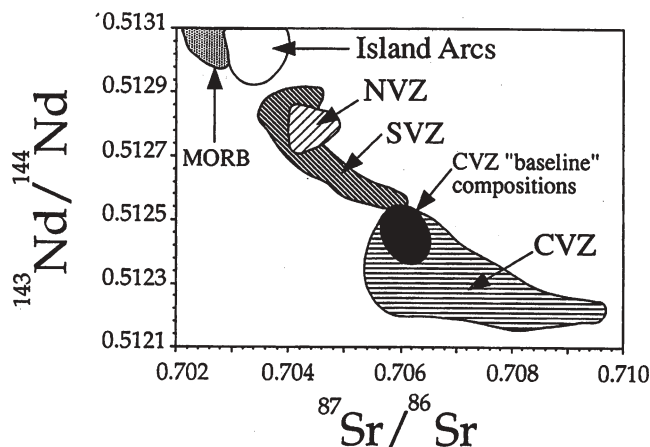


**Fig. 5.31.** Sr versus Nd isotopic compositions for magmas erupted from volcanoes in different Andean arc segments (Davidson *et al.* 1991). The figure illustrates the isotopic differences between SVZ and CVZ volcanoes, compared to MORB and oceanic island arc volcanoes, and indicates the enriched Sr and Nd isotopic composition of 'baseline' parental magmas for volcanic rocks in the CVZ. This 'baseline' composition is produced either by lower crustal MASH processes (Davidson *et al.* 1991) or subcrustal mantle source region contamination (Stern 1991b).

parental magmas subsequently evolve at shallower levels through assimilation–crystallization processes involving upper crust and magma mixing, which in both cases were restricted to end-members of low isotopic contrast. However, lack of correlated variations in isotopic compositions and increasing SiO<sub>2</sub> content argues against such combined assimilation–crystallization processes, and is consistent instead with the generation of CVZ parental magmas with enriched 'baseline' isotopic compositions resulting from modification of the subcrustal mantle source by subducted crust and sediment (Figs 5.29 & 5.30; Stern 1988, 1990a, 1991b, c).

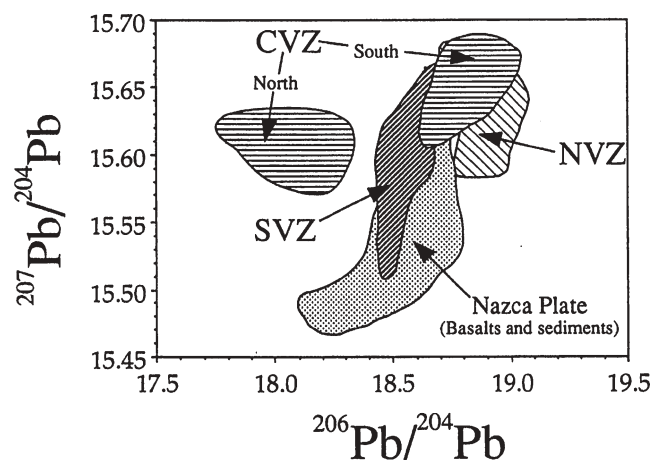


**Fig. 5.32.** Pb isotopes for volcanic rocks from different segments of the Andean arc (Davidson *et al.* 1991). The different Pb isotopic compositions of north and south CVZ volcanic rocks depend in part on the isotopic composition of the basement they have erupted through.

Unfortunately, because of the lack of basalts in this segment of the Andean arc, which may in itself be an indication of extensive subarc source-region contamination below the CVZ, the degree to which the baseline composition of magmas generated in the subarc mantle below the CVZ has been affected by source-region contamination is difficult to evaluate. Nevertheless, a number of different lines of evidence indicate that subduction erosion and source-region contamination play an important role in determining the baseline isotopic and trace-element composition of mantle-derived mafic magmas below the CVZ of northern Chile. Most significant is the fact that some primitive mantle-derived mafic CVZ magmas with enriched isotopic signatures also have high Mg numbers and Cr and Ni contents, implying that they erupted through the thick Andean crust without significant intracrustal assimilation (Kay



*et al.* 1999). These include samples from the San Francisco and Icahuasi volcanoes in the main volcanic line of the southern part of the CVZ, and from southern and central Puna backarc mafic lavas (Dérulle 1991), which all have  $^{87}\text{Sr}/^{86}\text{Sr}$  ratios of 0.705 to 0.707, and  $\epsilon_{\text{Nd}} < 1$ , within the range of CVZ 'baseline' compositions (Fig. 5.31). Kay *et al.* (1999) argue that these enriched isotopic signatures in the most primitive mafic magmas are best interpreted as resulting from subcrustal processes such as subduction erosion and mantle source-region contamination. Macfarlane (1999) also concludes that Pb isotopic compositions of both northern Chile ores and CVZ volcanic rocks result from subduction of sediment into the subarc mantle magma source region.

Rogers & Hawkesworth (1989) demonstrated that enriched baseline isotopic signatures in magmas with increasingly high Sr content started to develop during the Miocene as the magmatic belt migrated eastward to its current position. They argue that these trends are inconsistent with contamination at crustal levels in which plagioclase is stable. They concluded instead that these signatures are due to increasing involvement of ancient enriched subcontinental lithospheric mantle as magmatism migrated eastward. Stern (1990a) argued that these same trends may be produced by increased subduction erosion and subarc mantle magma source-region contamination (Fig. 5.29) as a result of both flattening of subduction angle and decreasing sediment supply to the trench due to the increasingly arid conditions in northern Chile that began during the Miocene. He concluded that there is a good temporal correlation between increased subduction erosion, source-region contamination, and the increased importance of crustal components in CVZ magmas.

#### AVZ petrography, geochemistry and petrogenesis

AVZ volcanic rocks include only andesites and dacites, and no basalts, basaltic andesites or rhyolites have been erupted from these volcanoes (Stern *et al.* 1976b, 1984c; Stern & Kilian 1996; Orihashi *et al.* 2004). The essential mineralogy of all the AVZ andesites and dacites involves pyroxenes + amphibole + plagioclase. Biotite occurs only in the andesites and dacites of the three northernmost AVZ volcanoes (Stern 1990b; Stern & Kilian 1996). Cook Island and Mt Burney andesites contain mantle-derived clinopyroxene ± olivine xenocrysts (Stern & Kilian 1996). The presence of both a greater proportion of crustal xenoliths and larger, more complexly zoned phenocrysts is observed in AVZ volcanic rocks from south to north, suggesting an increasing importance of near-surface magma chamber processes such as slow cooling and crystallization, magma mixing, wall-rock assimilation, and volatile degassing.

The AVZ andesites and dacites have adakitic chemical features (Stern *et al.* 1984c; Futa & Stern 1988; Stern & Kilian 1996), with  $\text{SiO}_2 > 56$  wt% and  $\text{Al}_2\text{O}_3 > 15$  wt%, relatively high Mg#, low HREE ( $\text{Yb} < 1.9$  ppm) and  $\text{Y} < 18$  ppm, high Sr > 400 ppm and  $\text{Sr}/\text{Y} > 40$  (Fig. 5.33), and positive Sr and Eu anomalies. These characteristics have been interpreted to reflect the presence of residual garnet, amphibole and pyroxene, but little or no olivine and plagioclase in the source region. AVZ andesites and dacites also have low concentrations of HFSE, including  $\text{TiO}_2$ , which is a common feature of both adakites and typical convergent plate boundary magmas.

The AVZ occurs in an area of relatively thin crust (< 35 km), and the source of AVZ adakites is thus likely to be subducted oceanic basalt, recrystallized to garnet-amphibolite or eclogite (Stern & Kilian 1996; Kilian & López-Escobar 2000). Geothermal models indicate that partial melting of the subducted oceanic crust is probable below the AVZ due to the slow subduction rate and the young age of the subducted oceanic lithosphere. However, other chemical characteristics, such as LILE ( $\text{K}_2\text{O}$ , Rb, Ba and Cs) and LREE content, LREE/HREE and LILE/LREE ratios, and Sr, Nd (Fig. 5.34), Pb, Hf and O isotopic compositions, which may reflect source composition

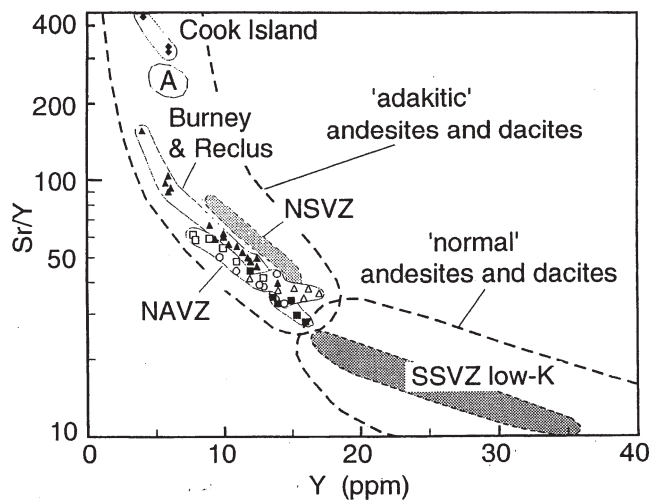


Fig. 5.33. Sr/Y versus Y for sample from the Andean AVZ (Stern & Kilian 1996). Fields for 'adakitic' and 'normal' andesites are taken from Defant & Drummond (1990). The type adakite from Adak island is marked as A. Fields for NSVZ andesites are from Futa & Stern (1988) and for SSVZ low-K basalts from López-Escobar *et al.* (1993).

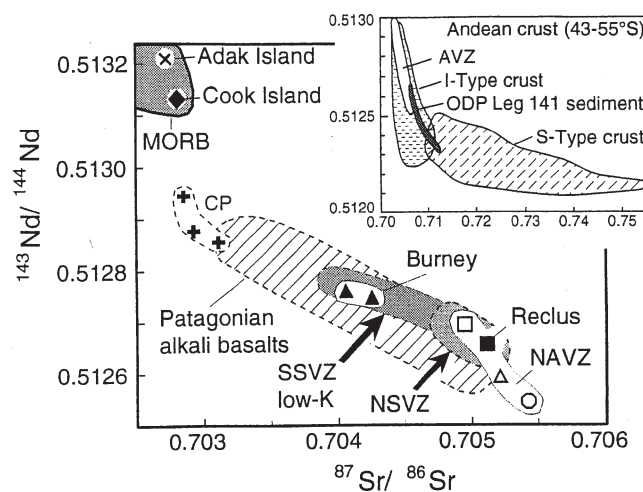


Fig. 5.34.  $^{143}\text{Nd}/^{144}\text{Nd}$  versus  $^{87}\text{Sr}/^{86}\text{Sr}$  for samples from the Andean AVZ (Stern & Kilian 1996), compared to fields for MORB, Patagonian plateau basalts (Stern *et al.* 1990), Cerro Pampa and Adak Island adakites, NSVZ andesites and SSVZ low-K basalts. Inset compares AVZ samples to southern South American metamorphic basement (S-type), Patagonian batholith (I-type), and Chile trench sediments (Kilian & Behrmann 2003).

rather than source mineralogy, vary significantly between, but not within, individual centres (Stern *et al.* 1984c; Futa & Stern 1988; Stern & Kilian 1996; Hattori *et al.* 2005). Although some Cook Island adakites contain xenoliths of granite from the Patagonian batholith (Dreher *et al.* 2005), others are xenolith-free and have MORB-like isotopic compositions (Stern & Kilian 1996; Sigmarsson *et al.* 1998; Bindeman *et al.* 2005; Hattori *et al.* 2005). The other AVZ centres to the north have isotopic compositions suggesting a greater proportion of subducted sediment or assimilated continental crust involved in their genesis.

To explain the origin and evolution of these AVZ adakitic andesites and dacites, Stern & Kilian (1996) proposed a multi-stage four-component model involving subducted MORB metamorphosed to garnet-amphibolite or eclogite, subducted

sediment, mantle wedge and continental crust. According to this model, the proportions of the different source materials involved in the genesis of AVZ magmas vary significantly from south to north. The adakitic andesites from Cook Island volcano, where subduction is most oblique (Fig. 5.24), can be modelled by small degrees (2–4%) of partial melting of eclogitic MORB with little participation of subducted sediments, yielding a primary magma that interacts to only a very limited extent with the overlying mantle and continental crust. In contrast, models for the magmatic evolution of other AVZ andesites and dacites located between 49°S and 52°S, where subduction is more orthogonal (Fig. 5.24), require melting of a mixture of MORB and subducted sediment, followed by interaction of this primary melt with the overlying mantle and the continental crust. Based on geochemical data for Chile Trench sediments (Kilian & Behrmann 2003), these models suggest that the input of subducted sediments is variable, between 0 and 20% for the AVZ volcanoes, and that intracrustal AFC processes and the mass contribution from the continental crust become more significant northwards in the AVZ as the angle of convergence becomes more orthogonal.

### Backarc alkali plateau basalts (M.A.S. & C.R.S.)

Pleistocene and Holocene backarc volcanism occurs to the east of the Andean arc between latitudes 34°S and 52°S (Skewes & Stern 1979; Baker *et al.* 1981; Stern *et al.* 1990). Pleistocene and Holocene backarc volcanic activity, which generally consists of alkali basalt lava flows erupted from small monogenetic spatter and scoria cones, forms the youngest part of the Patagonian plateau basalts. The Patagonian plateau basalts are located

dominantly in Argentina, but the western parts of this volcanic province, including Pleistocene and Holocene cones and flows, also occur in southernmost Chile (Fig. 5.24), specifically along the western edge of Meseta Vizcachas exposed in Cordillera Baguales (50.5°S, 72.5°W; Muñoz 1981; Kilian & Stern 2002), and in the Pali-Aike volcanic field (51–52°S, 69–71°W; Skewes & Stern 1979; D'Orazio *et al.* 2000), which straddles the Chile–Argentina border close to the Atlantic coast just north of the Magellan Straits.

### Geological and tectonic setting

Pleistocene and Holocene backarc volcanic activity in southern Chile forms the youngest part of the Patagonian plateau lavas located south of the locus of subduction of the Chile Rise at 46°S (Fig. 5.24). The eastward extension of the Chile Ridge, which separates the Nazca and Antarctic plates, was subducted below southernmost Patagonia beginning in the Miocene (Ramos & Kay 1992; Gorrington *et al.* 1997; D'Orazio *et al.* 2000, 2001; Gorrington & Kay 2001; Kilian & Stern 2002; Espinoza *et al.* 2005; Guivel *et al.* 2006). Neogene backarc volcanic activity in southernmost Patagonia has been attributed to the subduction of the Chile Ridge, which resulted in the opening of an asthenosphere slab-window between the relatively rapidly down-going Nazca Plate and the more slowly subducting Antarctic Plate (Fig. 5.35).

The Pali-Aike volcanic field occurs in the area of the Magellan basin, which began subsiding in the Jurassic in conjunction with the opening of the southern Atlantic Ocean. The continental crust underlying the Pali-Aike basalts consists of Jurassic silicic volcanic rocks of the Tobifera Formation (Bruhn *et al.* 1978), and Jurassic to Miocene marine and continental sedimentary rocks deposited on pre-Andean

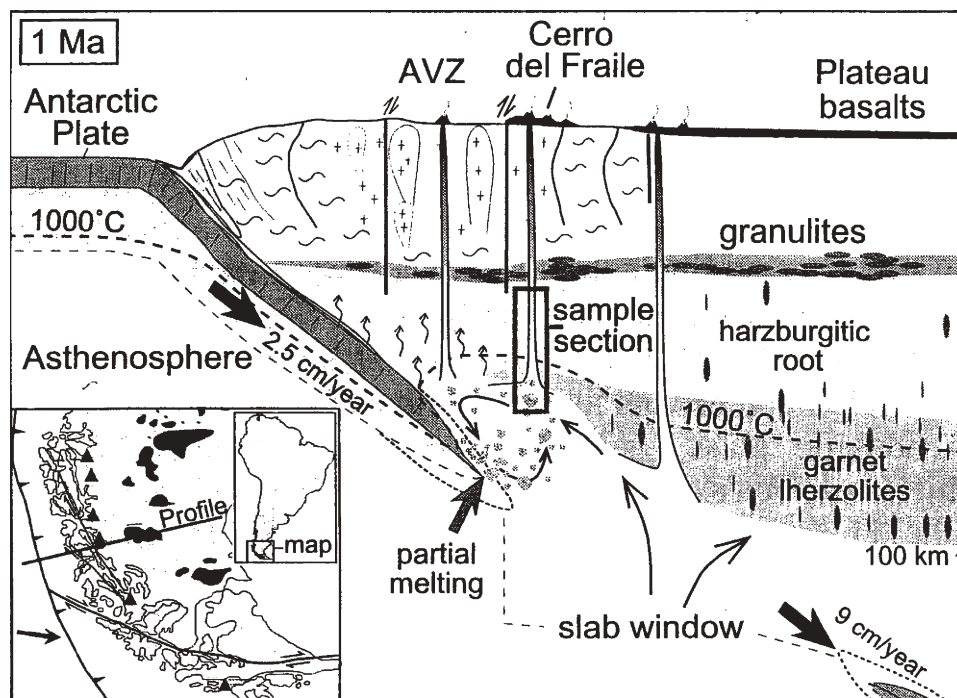


**Fig. 5.35.** Cross-section through the mantle below the AVZ, Meseta Vizcachas (Cerro del Fraile) and Pali-Aike (plateau basalt) field, modified from Kilian & Stern (2002), illustrating the slab-window model for backarc alkali basalt volcanic activity. Meseta Vizcachas alkali basalts have incorporated slab-derived components (Stern *et al.* 1990), and contain mantle xenoliths with metasomatic geochemical features resulting from the influx of slab-derived fluids and melts (Kilian & Stern 2002; Wang *et al.* 2007). These components are derived from the leading edge of the subducted Antarctic Plate. In contrast, Pali-Aike basalt and the metasomatized mantle xenoliths they contain do not have any evidence of slab-derived components (Stern *et al.* 1990, 1999), but were derived entirely from subslab asthenosphere rising up through the slab-window and interacting with the lower continental mantle lithosphere.



metamorphic basement. Meseta Vizcachas basalts occur along the western margin of this basin, above Cenozoic continental sediments uplifted along the eastern margin of the Austral Basin fold-and-thrust belt.

### *Pali-Aike volcanic field*

The Pali-Aike volcanic field is >50 km wide and >150 km long. It consists of basaltic lava flows extruded from hundreds of monogenetic spatter and scoria cones (Figs. 5.36 & 5.37), and tuff rings associate with numerous maars (Fig. 5.38). Cones and maars are orientated along NE–SW and NW–SE lineations. The field takes its name from the Pali-Aike spatter cone, an archaeological site within which a cave formed along the inner wall of the cone was found to contain evidence of human occupation dating back >10 000  $^{14}\text{C}$  years BP (Bird 1938, 1988).

The Pali-Aike field formed between 3.8 Ma and the Holocene, but has not had historic activity. Three different units are recognized in the field (Skewes 1978; Skewes & Stern



**Fig. 5.38.** Laguna Ana maar and surrounding tuff ring, behind another unnamed maar partially filled by a younger lava flow. These are two among many such maars in the Pali-Aike volcanic field. Photo taken by C.R. Stern.



**Fig. 5.36.** The Pali-Aike spatter cone viewed from the east, one of hundreds of such cones in the Pali-Aike volcanic field. A cave in the inner wall of the cone is an archaeological site found to contain evidence of human occupation dating back >10 000  $^{14}\text{C}$  years BP (Bird 1938, 1988). Photo by C.R. Stern.



**Fig. 5.37.** The Cerro Diablo scoria cone and associated lava flows, the youngest active volcano in the Pali-Aike volcanic field, located just east of the older Pali-Aike cone. Photo by C.R. Stern.

1979; D'Orazio *et al.* 2000). The oldest unit forms an extensive area of plateau-like basaltic lavas approximately 100 m thick. The two younger units, which are spatially more restricted, are both post-glacial (<1 million years). The partially eroded and aeolian sediment-covered Pali-Aike cone (Fig. 5.36) and Laguna Ana maar (Fig. 5.38) both belong to the second unit in the Pali-Aike field, estimated to have formed between 130–17 ka based on K–Ar ages (Meglioli 1992). The youngest lava flows are associated with the Cerro Diablo scoria cone (Fig. 5.37). Based on their fresh glassy appearance and lack of any aeolian soil cover, these flows are certainly <10 000 years old.

Pali-Aike basalts are nepheline normative alkali olivine basalts, with notably high  $\text{TiO}_2$  content and intraplate geochemical characteristics similar to some oceanic islands and lacking any evidence for the incorporation of subducted components into their source (Skewes & Stern 1979; Stern *et al.* 1990). Their chemical compositions are consistent with derivation by low degrees of melting of mantle asthenosphere, either due to subduction-induced thermal and mechanical perturbation (Stern *et al.* 1990), or rising through a slab-window (Fig. 5.35; D'Orazio *et al.* 2000; Kilian & Stern 2002).

Pali-Aike basalts contain ultramafic xenoliths of mantle origin, including a unique suite of garnet-bearing peridotite xenoliths, which generally are not found in alkali basalts (Skewes & Stern 1979; Stern *et al.* 1986, 1989, 1999). Mineral chemistry geothermometry and geobarometry for these xenoliths indicate that the continental lithosphere below Pali-Aike is relatively thin (<100 km; Figs 5.35 & 5.39). Major and trace-element, and isotope chemistry of Pali-Aike garnet peridotites indicates that the deeper portions of this lithosphere consist of fertile garnet lherzolites with trace-element and isotopic compositions similar to the mantle source of mid-oceanic ridge basalts (Fig. 5.35). The data imply the absence of a deep, low-density, olivine-rich mantle root below the Palaeozoic–Mesozoic crust of southernmost South America such as has been inferred below Archaean cratons (Stern *et al.* 1999). Pali-Aike garnet peridotites have been both modally and cryptically metasomatized by fluids genetically related to the alkali host basalts. These xenoliths, most of which occur in tuff rings associated with maars, have been transported to the surface at velocities estimated to be between 1 and 6 m/s (Selverstone & Stern 1983; Demouchy *et al.* 2006), similar to velocities estimated for the emplacement of kimberlite magmas.



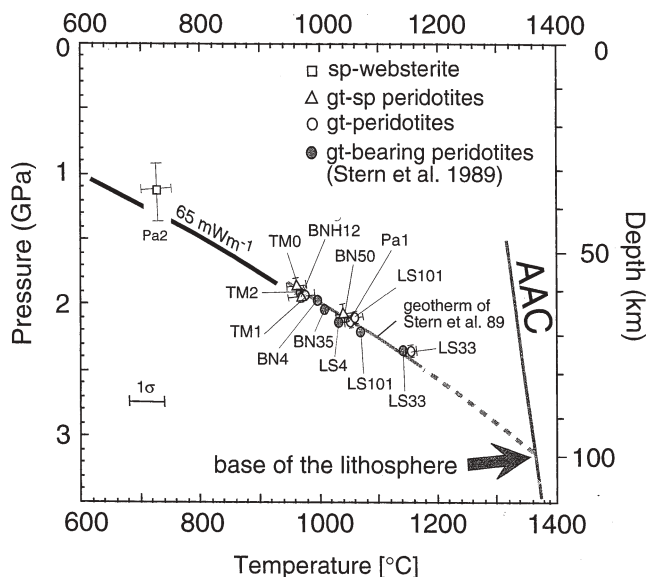


**Fig. 5.39.** Geothermal gradient in the mantle lithosphere below the Pali-Aike volcanic field in southernmost South America as determined by mineral geothermometry and geobarometry on peridotite xenoliths contained in the Pali-Aike basalts (Stern *et al.* 1986, 1989, 1999). The figure illustrates that the lithosphere below this region of continental crust is relatively thin (< 100 km; Fig. 5.35), as indicated by the depth of intersection of the geotherm with the adiabatic upwelling curve (ACC).

#### Quaternary volcanism in Cordillera Baguales

The deeply eroded, *c.* 1000-m-thick western edge of Meseta Vizcachas (Fig. 5.40) forms Cordillera Baguales along the border between Chile and Argentina at 50.5°S latitude (Fig. 5.25; Muñoz 1981). Lavas from the western margin of Meseta Vizcachas at Cerro del Fraile in Argentina are interbedded with fluvial-glacial sediments and have been dated to 1–2 Ma (Fleck *et al.* 1972). In Argentina, Meseta Vizcachas is covered by numerous small spatter and scoria cones, presumably younger than the eroded lavas dated at Cerro del Fraile. Sills and dykes are exposed within the deeply eroded lava cliffs of Cordillera Baguales.



**Fig. 5.40.** Cordillera Baguales, the deeply eroded western edge of the Meseta Vizcachas Pliocene, Pleistocene and Holocene plateau basalts. Photo taken by C.R. Stern.

Petrochemically, Cordillera Baguales is formed by olivine basalts with chemical affinities transitional between alkaline and subalkaline (Muñoz 1981). Unlike Pali-Aike basalts, Cordillera Baguales basalts have trace-element characteristics such as high LILE/LREE (for example Ba/La > 15) and LREE/HFSE (for example La/Nb > 1) suggesting incorporation of subducted components into their mantle source (Stern *et al.* 1990; Kilian & Stern 2002). Cordillera Baguales basalts also contain mantle xenoliths which have been metasomatized by adakite-like melts and fluids derived from subducted oceanic lithosphere (Kilian & Stern 2002), including subducted oceanic sediment (Wang *et al.* 2006). Kilian & Stern (2002) attribute the addition of these components to the mantle source region of Cordillera Baguales basalts to melting of the leading edge of the down-going Antarctic Plate as the slab-window began to close under this region, which is only 25 km east of the Reclus AVZ volcano (Fig. 5.35).

#### Chile Ridge and Chile triple-junction volcanism (L.E.L. & C.R.S.)

Several submarine volcanic centres are located along the NW–SE trending Chile Ridge, which is formed by relatively short active ocean-floor spreading segments bounded by NE–SW fracture zones. The Chile Ridge is being subducted beneath the South American Plate west of the Taitao Peninsula (46°S; Figs 5.1, 5.8 & 5.41). Dredged rocks from the Chile Ridge are mainly MORB-type basalts, but they show a wide spectrum of geochemical signatures, in particular trace-element ratios (Klein & Karsten 1995; Karsten *et al.* 1996). Far from the trench, MORB-like signatures predominate, but near the margin arc-like trace-element signatures are observed. These arc-like geochemical characteristics in Chile Ridge basalts are considered to reflect contamination of a depleted N-MORB source mantle with slab-derived components due to slab break-up or shearing in conjunction with subduction of this young buoyant lithosphere, and subsequent entrainment of these slab components into the subridge mantle (Klein & Karsten 1995; Karsten *et al.* 1996; Guivel *et al.* 2003, 2006).

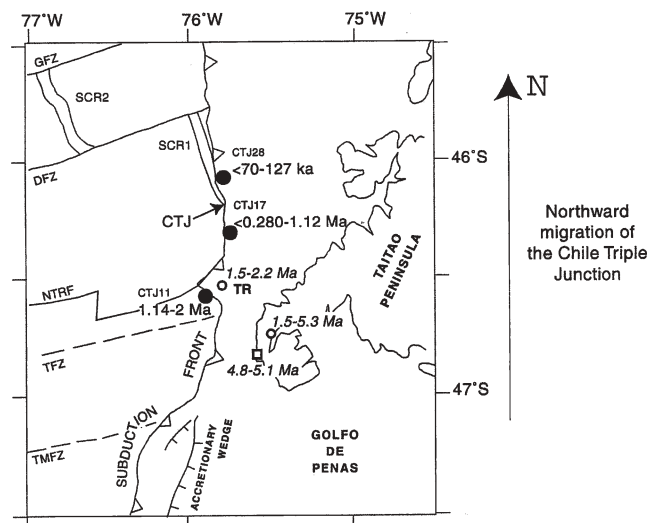


**Fig. 5.41.** Map of the location of the Pliocene and Quaternary calcalkaline magmatic rocks in the vicinity of the Chile triple-junction (CTJ) modified from Guivel *et al.* (2003, fig. 8). SCR1 and SCR2 are segments of the Chile Ridge offset by various fracture zones. TR is the Taitao fore-arc ridge.

Moreover, in the area referred to as the synsubduction segment of the Chile margin (Bourgeois *et al.* 2000), Pleistocene–Holocene (70 ka to 2 Ma) calcalkaline basaltic andesites and dacites, with subduction-related geochemical characteristics, have been dredged from both the Chile Trench and the Taitao ridge (TR, Fig. 5.41; Guivel *et al.* 2003). Chemically similar Late Miocene, Pliocene and Pleistocene igneous rocks also occur in the Cabo Raper plutonic suite (4.8–5.1 Ma; Guivel *et al.* 1999) and the volcanic–sedimentary sequence of the Chile Margin Unit (1.5–5.3 Ma; Bourgeois *et al.* 1993, 1996) on the forearc of Peninsula Taitao. The age of these volcanic rocks gets younger towards the present-day triple-junction.

### Petrology and petrogenesis

Among the dacites, both low- and high-silica varieties occur. They are both interpreted to be derived from relatively shallow hydrous melting of subducting oceanic basalts and associated sediments under high thermal conditions (Fig. 5.42). Low-silica

dacites show chemical characteristics of adakitic slab melts, with depleted HREE abundances suggesting the occurrence of residual garnet in their source at depths of 25–45 km. High-silica dacites are less depleted in HREE and are interpreted to represent melts of MORB and sediment at even shallower depths of <25 km. Basaltic andesites have predominantly mantle-derived geochemical characteristics and are thought to result by mixing of dacite magmas with MORB-type liquids derived from a buried spreading ridge (Guivel *et al.* 2003). The high temperatures required to produce melting at shallow depths result from what has been referred to as a ‘blowtorch’ effect (Lagabrielle *et al.* 2000, 2004), caused by the back (south) and forth (north) migration of the triple junction due to the successive subduction of the short NW–SE Chile Ridge segments separated by NE–SW fracture zones (Fig. 5.41).

Various models have been suggested to explain the spatial proximity of these young volcanic rocks to the current trench axis. These include: (1) rise of their parent magmas from their source to the surface along the subduction thrust plane; (2) rapid tectonic erosion caused by ridge subduction (Fig. 5.42); or (3) changes in the geometry of the subducted slab, causing a steepening of subduction angle in response to mantle counterflow moving from the backarc towards the trench in the mantle wedge (Guivel *et al.* 2003).

### Intraplate oceanic volcanism: the Pacific volcanic islands of Chile (L.E.L. & C.R.S.)

Three separate clusters of islands in the southeastern Pacific are formed by intraplate oceanic volcanoes occurring along linear chains of seamounts on the Nazca Plate. These three clusters include (1) Easter, Salas and Gómez islands along the western edge of Salas and Gómez seamount chain, (2) San Félix and San Ambrosio islands along the eastern edge of this chain, and (3) Robinson Crusoe, Santa Clara and Alejandro Selkirk islands along the Juan Fernández seamount chain. These islands are the subaerial upper parts of large, nested and partially eroded stratovolcanoes.

Most of these islands had early Pliocene (*c.* 4–3 Ma) stages of submarine growth, Surtseyan pyroclastic deposits and dyke swarms that fed later subaerial volcanoes, some of them active in the Holocene. They also show advanced erosion, mainly related to sector-collapse processes. On a larger, tectonic-plate scale, they could represent the long-lived manifestations of mantle hot-spot plumes, the temporal evolution and petro-physical behaviour of which are still not well understood in the area of the southeastern Pacific. What is clear is that subduction of the aseismic ridges of which these islands form a part has important effects on the South American margin. For example, subduction of the Juan Fernández Ridge, from the Eocene to the present, may have produced changes in subduction angle (Yañez *et al.* 2001, 2002), affected coastal tectonics and the present pattern of seismicity of both outer-rise and forearc domains in central Chile (von Huene *et al.* 1997), and resulted in the genesis of giant Andean copper deposits in central Chile (Stern & Skewes 2005).

### Easter and Salas and Gómez islands

Easter Island (27°09'S, 109°23'W, 560 m) occurs 350 km east of the East Rift spreading ridge on the eastern margin of the Easter microplate, and near the western edge of a long chain of seamounts that also includes both Salas and Gómez Island (26°28'S, 105°22'W, 30 m) as well as more than 553 other cone-shaped or flat submarine seamounts recognized from high-resolution bathymetry (Rappaport *et al.* 1997).

Easter Island volcanic complex is formed by three coalescent volcanic centres (Rano-Kao, Poike and Terevaka-Tangaroa) and several superimposed pyroclastic cones and lava flows.

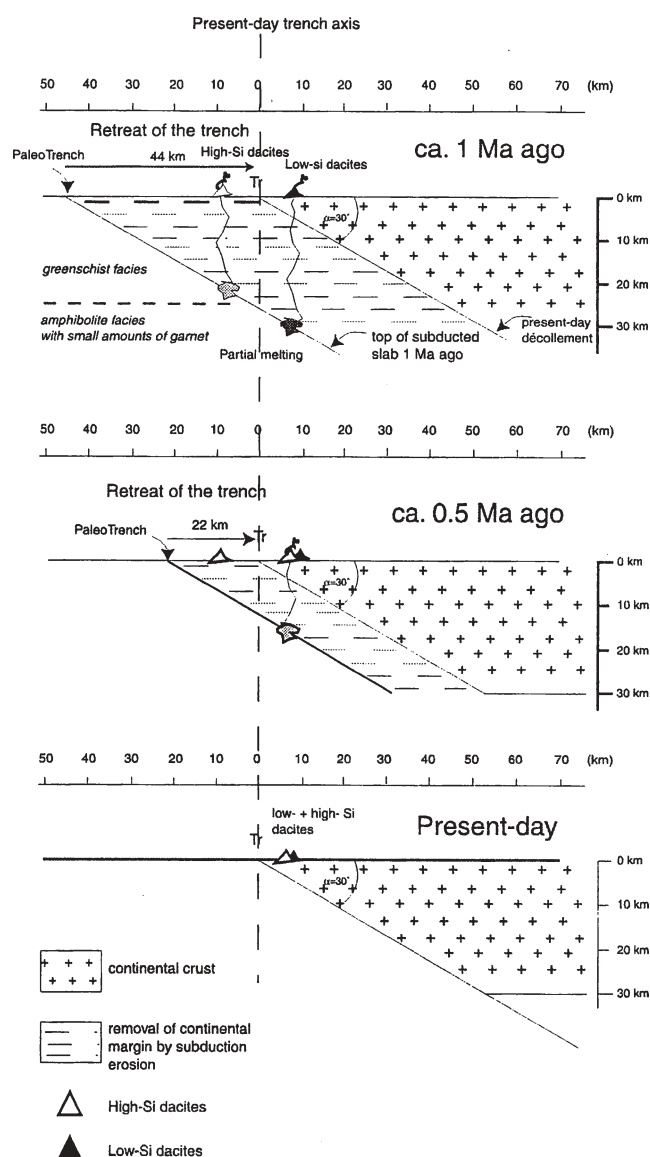


**Fig. 5.42.** Cross-sections, modified from Fig 11 in Guivel *et al.* (2003, fig. 11), illustrating the conditions of shallow slab melting to produce low- and high-silica dacites found in the synsubduction zone of the Chile triple-junction, and a geodynamic model involving high rates of subduction erosion (44 km in 1 million years) to bring these igneous rocks to their current near-trench axis position on the Taitao ridge.





**Fig. 5.43.** Outcrops of lavas along the NE coast of Santa Clara Island as viewed from Robinson Crusoe island. Photo taken by A. Díaz.

The nearly coeval Rano-Kao and Poike stratocones were built beginning in the Late Pliocene (*c.* 2.6 Ma). They are eroded, exposing thick volcanic successions with interbedded pyroclastic ejecta produced by phreatomagmatic eruptions. Late extrusion of rhyolitic domes occurred on the flanks of both Rano-Kao and Poike. K–Ar ages for Maunga Orito and Te Manavai domes associated with the Rano-Kao volcano are, respectively, 230 ka and 180 ka. Jet-black rhyolite obsidian occurs associated with a rhyolitic dome in Rano-Kao caldera.

The youngest volcanic centre is the Terevaka-Tangaroa volcano, a shield complex active since approximately 1.5 Ma. A thick pile of basaltic lavas was emitted from several fissure vents on this volcano. Possibly Holocene lavas erupted from several flank vents are the youngest evidence of activity at Easter Island. Historical reports and local myths suggest eruptions as recently as 2000 years ago.

#### *San Félix and San Ambrosio islands*

San Félix (26°17'S, 80°07'W, 193 m) and San Ambrosio (26°20'S, 79°58', 479 m) islands, together with other small emerged lands such as the Peterborough Cathedral, are parts of huge shield volcanoes and perihelal centres located in the easternmost segment of the Salas and Gómez submarine volcanic chain. San Félix Island corresponds to a tuff-ring related to phreatomagmatic eruptions, which truncated an older alkaline shield volcano. Lava flows and pyroclastic deposits with fresh morphology cover the island. San Ambrosio island is also a remnant of a shield volcano where two uncomformable sequences are cut by vertical dykes dated to  $2.93 \pm 0.15$  Ma (Bonatti *et al.* 1977).

#### *Alejandro Selkirk and Robinson Crusoe islands*

Robinson Crusoe (33°3'S, 78°53'W, 915 m) and Alejandro Selkirk (33°45'S, 80°45'W, 1650 m) islands occur along the Juan Fernández Ridge (Fig. 5.1), a *c.* 900-km-long, east–west-trending volcanic chain of mostly submarine volcanoes. Alejandro Selkirk and Robinson Crusoe (Fig. 5.43) islands are remnants of ancient shield volcanoes. Alejandro Selkirk consists of a homoclinal lava sequence that yields K–Ar ages of  $0.85 \pm 0.30$  and  $1.3 \pm 0.3$  Ma (Booker *et al.* 1967). Robinson Crusoe island, in turn, has a heavily eroded profile where two uncomformable sequences can be recognized. They are cut by coalescent vertical dykes and some laccoliths around which has developed intense hydrothermal alteration. Marine

sedimentary deposits partially cover the island and record sea level rising during the Pleistocene (Valenzuela 1978). Booker *et al.* (1967) dated the lower lava sequence of Robinson Crusoe to between  $3.5 \pm 0.8$  and  $3.1 \pm 0.9$  Ma. Baker *et al.* (1987a) obtained  $4.0 \pm 0.2$  Ma for the same unit. Possible historical renewal of volcanic activity was suggested by Sutcliffe (1839) during Charles Darwin's expedition to the South Pacific area.

The Juan Fernández Ridge is supposed to be related to a mantle hot-spot, the present location of which would be west of Alejandro Selkirk island, below the vicinity of the Domingo and Friday seamounts (Farley *et al.* 1993; Devey *et al.* 2000), but these have not been dated. The present-day nearest-trench seamount (Monte O'Higgins) was dated as *c.* 8.5 Ma by  $^{40}\text{Ar}/^{39}\text{Ar}$  (von Huene *et al.* 1997). Although the subduction of the eastern extension of this ridge played an important long-term role in the Cenozoic evolution of the South American margin (Yañez *et al.* 2001, 2002; Stern & Skewes 2005), the precise track of the supposed plume-fed hot-spot volcanism remains unknown.

#### *Petrogenesis of Chilean oceanic islands*

Geochemical signatures of the volcanic rocks from Easter Island are mainly tholeiitic with scarce silica-poor alkaline varieties (Clark & Dymond 1977). Hekinian *et al.* (1996) have described a mixing of N-MORB and E-MORB characteristics for Easter Island, suggesting a mixing between Pacific mid-oceanic ridge and hot-spot sources, as might be expected from the proximity of Easter Island to the Pacific Ridge. Other young seamounts and submarine volcanic fields in the area, such as Ahu and Tupa, which may be related to the Easter Island hot-spot, exhibit similar chemical characteristics (Haase & Devey 1996).

Baker *et al.* (1987a) studied the transitions from tholeiitic to alkaline affinities in volcanic rocks from Robinson Crusoe and Alejandro Selkirk islands. They concluded that the chemistry of the early tholeiitic stage of formation of the islands resulted from a high degree of partial mantle melting, consistent with a steep geothermal gradient likely to be associated with a hot-spot. Later-stage alkaline rocks were derived by remelting of a source region previously subjected to small but variable degrees of partial melting and melt migration over a prolonged period. More recently, Devey *et al.* (2000), as a result of a study of the younger Domingo and Friday seamounts along the Juan Fernández Ridge, suggested melting of a MORB-like suboceanic harzburgite source modified by metasomatic reactions with  $\text{CO}_2$ -rich plume-melts, similar to the metasomatism related to the generation of kimberlitic magmas. They proposed that these plume-melts were derived from a source that included ancient recycled oceanic crust.

Gerlach *et al.* (1986) described the mantle heterogeneities beneath the Nazca Plate from Sr–Nd systematics, recognizing both EMI and EMII components as parental composition of some hot-spot volcanoes that follow distinct geochemical trends. In contrast, Devey *et al.* (2000) suggested that mixing of PREMA and HIMU mantle sources produced the isotopic variability observed among the various islands and seamounts along the Juan Fernández Ridge.

We thank E. Godoy and D. Morata for their constructive suggestions. D. Mitchell (University of Colorado) helped prepare some of the figures.